Litter decomposition is moderated by scale-dependent microenvironmental variation in tundra ecosystems

Authors:

Elise Gallois (1), Isla H. Myers-Smith (1), Gergana N. Daskalova (1), Jeffrey T. Kerby (2), Haydn J.D. Thomas (1) Andrew M. Cunliffe (3)

Affiliations:

1. School of GeoSciences, University of Edinburgh, Edinburgh, UK
2. Aarhus Institute of Advanced Studies, Aarhus University, Aarhus, Denmark
3. Department of Geography, University of Exeter, Exeter, UK

Orcid ID:

Elise Gallois, **0000-0002-9402-1931**

Isla Myers-Smith, **0000-0002-8417-6112**

Gergana Daskalova, **0000-0002-5674-5322**

Jeffrey Kerby, **0000-0002-2739-9096**

Haydn Thomas, **0000-0001-9099-6304**

Andrew Cunliffe, **0000-0002-8346-4278**

Abstract:

1. Tundra soils are one of the world's largest organic carbon stores, yet this carbon is vulnerable to accelerated decomposition as climate warming progresses. We currently know very little about landscape-scale controls of litter decomposition in tundra ecosystems, which hinders our understanding of the global carbon cycle.
2. Here, we examined how local-scale topography, surface air temperature, soil moisture and permafrost conditions influenced litter decomposition rates across a heterogeneous tundra landscape on Qikiqtaruk - Herschel Island, Yukon, Canada.
3. We used the Tea Bag Index protocol to derive decomposition metrics, which we then compared across environmental gradients, including thermal sum surface temperature data derived from fine-resolution microclimate data modelled from drone derived topographic data.
4. We found greater green tea litter mass loss and faster decomposition rates in wetter and warmer areas within the landscape, and to a lesser extent in areas with deeper permafrost active layer thickness.
5. Spatially heterogeneous belowground conditions (soil moisture and active layer depth) explained variation in decomposition metrics at the landscape-scale (> 10 m) better than surface temperature.
6. Surprisingly, there was no strong control of elevation or slope of litter decomposition. We also found higher decomposition rates on North-facing relative to South-facing aspects at microsites that were wetter rather than warmer.
7. *Synthesis*: Our results show that there is scale-dependency in the environmental controls of tundra litter decomposition with moisture playing a greater role than microclimate at local "plot" scales. Our findings highlight the importance and complexity of microenvironmental controls on litter decomposition in estimates of carbon cycling in a rapidly warming tundra biome.

Keywords:

decomposition, tundra, tea bag index, microclimate, climate change, ecosystem change, carbon cycling

Introduction:

Climate change could lead to heterogeneous ecosystem responses across microclimates

Northern latitudes are warming at three times the rate of the global average, alongside increased precipitation and permafrost thaw (Bintanja & Andry, 2017; AMAP, 2021; IPCC, 2021; Kaufman et al., 2009; AMAP, 2017; Xue et al., 2016). In response, trees and woody shrubs are shifting their distributions northward, and vegetation, particularly in shrubs, grasses and sedges, is increasing across tundra landscapes (Chapin et al., 2005; Elmendorf, Henry, Hollister, Björk, Boulanger-Lapointe, et al., 2012; Holtmeier & Broll, 2005; Myers-Smith, Forbes, et al., 2011; Myers-Smith & Hik, 2018). Warming temperatures are also contributing to increasing decomposition rates in the Arctic, and higher rates of carbon cycling (Aerts, 2006; Hobbie, 1996; Mekonnen et al., 2021). The rate and magnitude of both above and belowground ecosystem changes are heterogeneous across the tundra, and may partly be explained by local environmental variation, for example in soil moisture content (Ackerman et al., 2017; Bjorkman et al., 2018; Elmendorf, Henry, Hollister, Björk, Bjorkman, et al., 2012; Myers-Smith et al., 2015; Scharn et al., 2021). However, despite a growing understanding of the diverse ecological responses to climate change, the role of microenvironments and microclimates in mediating tundra carbon cycling is not yet clear, and there are likely many interactions between vegetation community change and decomposition dynamics in cold environments (Aguirre et al., 2021; Björnsdóttir et al., 2021; Kemppinen, Niittynen, le Roux, et al., 2021; Kemppinen et al., 2021).

Climate change is altering the Arctic carbon cycle, but we don't know the role of microclimate

The Arctic tundra and boreal regions are some of the planet's largest carbon stores, with approximately 217±12 Pg of carbon stored in the top 30 cm of permafrost soils (Hugelius et al., 2014; Miner et al., 2022; Schuur et al., 2009). On a global scale, climate warming is predicted to accelerate decomposition rates and in turn trigger greater release of carbon into the atmosphere (Bond-Lamberty & Thomson, 2010; Crowther et al., 2016; Davidson & Janssens, 2006). With increased prevalence of leaf litter material available to decompose, there is potential for a positive feedback loop whereby increased decomposition will generate increased levels of carbon from this newly available leaf litter (Hobbie et

al., 2000). A negative feedback effect could occur whereby an increase in recalcitrant litter due to increasing shrub abundance, could lead to a net deceleration of decomposition and net increase in carbon storage across the tundra (Cornelissen et al., 2007a). Vegetation type - and thus litter quality, which we define as the litter's quality as a resource for microbes - is a strong predictor of decomposition (Aerts, 2006; Aerts et al., 2012; Buckeridge et al., 2010; Thomas et al., in review). For example, graminoid species commonly produce more labile litter, while many shrub species often produce more recalcitrant woody litter (Cornelissen et al., 2007a; Shaver et al., 2006). However, landscape-scale variation in Arctic vegetation and permafrost disturbances are not reliably captured (more frequently underestimated) by macro-scale observations (Assmann et al., 2020; Berner et al., 2020; Myers-Smith et al., 2020; Siewert & Olofsson, 2020). We thus need to quantify the heterogeneity of the relationship between local environmental conditions and litter decomposition metrics across the tundra to better estimate future carbon losses (Bradford et al., 2014).

Info Box: Microclimate terminology & spatial scaling

Spatial and temporal scales have long been considered a key issue for ecologists (Levin 1992). Field-based monitoring methods are often used to derive our broad-scale ecological predictions based on observations from limited sample sizes, and narrow domains of scale. Local above- and below-ground climate conditions vary across space. However, limited field observations of these variables cannot capture potentially meaningful local heterogeneity across a landscape and through time, particularly when low-resolution gridded climate data does not represent the climatic conditions occurring at the scale of the biological processes of interest (Bütikofer et al., 2020). The relative importance of microclimate versus regional macroclimate as an abiotic driver of ecological processes is increasingly appreciated in the literature (e.g., Lembrechts & Nijs, 2020; Niittynen et al., 2020), with more and more studies collecting thorough abiotic measurements across spatially heterogeneous tundra landscapes (Lembrechts et al., 2022; Rixen et al., 2022). However, consistent definitions of microclimate and microenvironment are not widely used in terms of both scientific classification and spatial extent. Here, we define 'microenvironment' as an umbrella term for highly localised abiotic and biotic conditions, including 'microtopography' (highly localised elevation, slope and aspect), vegetation community, and

113 'microclimate' (highly localised above- and below-ground temperature and soil moisture conditions).
114 Further to these classifications, we define the 'macro' scale as encompassing > 10s of kilometres square,
115 the 'landscape' scale as encompassing 0.1 - 10 kilometres square, and 'micro' scale as the highly local
116 < 10 m square scale. We refer to the plot-scale to indicate variation within our spiral plots in this study,
117 but acknowledge that the plot-scale will vary across studies according to the experimental design.
118
119 ***Abiotic controls on decomposition rates may vary in importance across spatial scales***
120 At the macro scale (10s of kms), litter decomposition is strongly influenced by abiotic conditions.
121 Among the different abiotic factors, air temperature is a key driver of decomposition, both globally and
122 within tundra ecosystems, though surface temperatures operating at the scale of tundra plant organisms
123 may be a stronger driver (Bütikofer et al., 2020; Hobbie, 1996; Sierra et al., 2015). Based on macro-
124 scale observations, we may therefore expect decomposition rates to increase across tundra regions
125 parallel to climate warming (Aerts, 2006; Crowther et al., 2016; Davidson & Janssens, 2006). In
126 contrast, at the landscape scale (0.1 - 10 kms) and at local scales (i.e., < 10 m), variables such as soil
127 moisture and active layer depth are highly variable (Ackerman et al., 2017; Bjorkman et al., 2018; Yi
128 et al., 2018; Zona et al., 2011) and may mediate decomposition rates. We do not know the extent to
129 which different tundra litter types are controlled by soil conditions versus surface temperatures, or at
130 which spatial thresholds an environmental variable becomes a reliable predictor of decomposition
131 characteristics.
132
133 ***The Tea Bag Index protocol reveals complexity of temperature and soil moisture as decomposition drivers***
134 Litter and substrate quality is also a key determinant of decomposition metrics (Cornwell et al., 2008).
135 Attempts to segregate the influence of environmental variables on decomposition metrics are therefore
136 often confounded by variation in substrate characteristics. One tool that has been used to address this
137 issue is the Tea Bag Index - a standardised protocol in which rooibos and green teas are used as a proxy
138 for naturally occurring recalcitrant and labile litter types, and their relative mass loss after a period of
139 burial is used to calculate decomposition rates (Keuskamp et al., 2013). While the protocol involves
140 using non-indigenous litter, it enables comparison across, and within, biomes, and experiments suggest

that the leaching of the tea bags are comparative between soil types, and are therefore reliable and stable proxies of local decomposition (Blume-Werry et al., 2021). In tundra environments, experiments using the Tea Bag Index (TBI) have indicated that soil temperature is the most accurate predictor of decomposition rates at the regional scale, but soil moisture conditions may actually be a stronger driver of litter decomposition on a site-b(Björnsdóttir et al., 2021)y-site basis (Thomas et al., in review; Walker et al., in prep).

The TBI protocol has also been implemented with warming manipulations to further investigate the potentially interacting microenvironmental drivers of decomposition. Sarneel et al. (2020) found stabilisation rates (a proxy for the amount of undecomposed litter after a period of litter burial) were more strongly driven by soil moisture than warming treatments - indicating that moisture conditions could be inhibiting decomposition. Björnsdóttir et al. (2021) observed higher decomposition rates under experimental warming conditions. They found that areas with vegetation shifts associated with warming also had higher decomposition rates, indicating indirect long term effects of warming, potentially as a result of increased litter input and associated changes in localised microbial communities (Björnsdóttir et al. 2021). The replicable nature of the TBI protocol, and its past success as a proxy of tundra decomposition traits, makes this an ideal tool for untangling the environmental drivers of decomposition across contrasting spatial scales.

Microenvironmental conditions interact with each other, and with biotic controls on decomposition

Abiotic conditions such as temperature and soil moisture and biotic variables such as vegetation types could likely interact with each-other to control decomposition. Decomposition rates are generally higher in wetter (though not saturated) soils, likely due to increased soil microbial and detritivore activity (Aerts, 2006; Buckeridge et al., 2010; Murphy et al., 1998; Rinnan et al., 2008; Swift et al., 1979; Thakur et al., 2018; Waring & Schlesinger, 1985; Thomas et al. in review; Walker et al., in prep). Experiments demonstrate greater decomposition with warming in tundra ecosystems with variation across vegetation types (Sarneel et al. 2020; Björnsdóttir et al. 2021). However, warming temperatures often lead to increased evapotranspiration in soils and therefore can also reduce rates of decomposition

(Rinnan et al., 2008; Sjögersten & Wookey, 2004), although this trend may be moderated in part by increased precipitation across northern latitudes (Sierra et al., 2015). Although labile litters, which are not as molecularly complex, decompose more rapidly (Davidson & Janssens, 2006), recalcitrant litters are also sensitive to soil moisture content and temperature (Suseela et al., 2013). To reliably predict future decomposition changes, it is important to consider the potentially interactive effects between these spatially variable drivers - and in particular disentangle the spatial scales at which these meaningful interactions operate to control long-term decomposition trends.

Earth-system models do not capture variability across heterogeneous tundra landscapes

Small adjustments to Earth-system models that simulate carbon balances can cause substantial changes in predicted future carbon storage and carbon losses (Carey et al., 2016; Crowther et al., 2016; Van Gestel et al., 2018). Local site-specific abiotic conditions explain ~73% of variation in global decomposition, while macroclimate data explain only ~28% (Bradford et al., 2014). As tundra ecosystems exhibit heterogeneity in both in vegetation patterning in above- and below-ground environmental conditions, we may expect to see variance in decomposition explained by regional macroclimate, and some explained by landscape-specific conditions (Ackerman et al., 2017; Bjorkman et al., 2018; Elmendorf, Henry, Hollister, Björk, Bjorkman, et al., 2012; Myers-Smith et al., 2015). A remaining question is therefore to what extent does decomposition, and thus carbon cycling, vary across landscapes that span multiple environmental gradients.

In this study, we investigated the spatial patterning and drivers of litter decomposition across a heterogeneous tundra landscape, spanning above- and below-ground microenvironmental gradients. We derived comparable litter mass loss metrics across multiple plots on Qikiqtaruk - Herschel Island, Yukon Canada. We collected local belowground micro-environmental data (soil moisture and active layer thickness). We used unoccupied aerial vehicle (hereafter drones) surveys to collect fine-resolution topographic data to model and analyse the varying effects of aboveground (surface microclimate) drivers on litter decomposition. We asked the following research questions: **(1) How do microclimate, microtopography and soil conditions vary spatially across a tundra landscape? (2) How does**

microtopography, microclimate, soil moisture and active layer thickness relate to litter decomposition? And, (3) do surface microclimate and below-ground microenvironment drivers interact to influence litter decomposition?. We tested the following hypotheses. 1) Mass loss is greater, and decomposition rates faster, in warmer and wetter areas and where permafrost active layers were deeper. And, 2) litter decomposition is greater at lower elevations in wetter soils, and on warmer south-facing slopes. Finally, we investigated the spatial patterning of both decomposition metrics and these environmental variables to determine whether the relationships between heterogeneous above- and below-ground environmental variables and carbon cycling are scale-dependent.

Methods & Materials:

We conducted our experiment on Qikiqtaruk - Herschel Island (69.6°N, -138.9°E) on the Arctic coast of the Yukon Territory, Canada. The undulating terrain and heterogeneous land cover at this site were ideally suited to test our research questions.

Study site

Qikiqtaruk has a maximum elevation of 183 m above sea level and is underlain entirely by ice-rich permafrost (Burn & Zhang, 2009). The general vegetation type is moist acidic shrub tundra (Myers-Smith & Hik, 2013), with two dominant vegetation communities across the island: 'Herschel' vegetation type, characterised by *Eriophorum vaginatum* tussocks and *Salix pulchra* canopies, and 'Komakuk' vegetation type, characterised by forb species (e.g., *Lupinus arcticus*), mosses, grasses, the willow species *Salix arctica* and *Salix glauca,* and *Dryas integrifolia* (Myers-Smith, Hik, et al., 2011). The spatial patterning of these vegetation communities is controlled by topography, soil conditions and physical disturbance (Obu et al., 2017). The vegetation across the island is sensitive to climate warming - canopy cover and plant heights have increased over the past two decades due to both community turnover and individual phenotypic responses (Myers-Smith et al., 2019). These changes correspond with trends observed across the surrounding western Canadian Arctic and more widely across the tundra

biome (Tape et al., 2006). The variable terrain and vegetation cover create heterogeneous microenvironmental conditions across the 1.5 km study transect (Fig. 1).

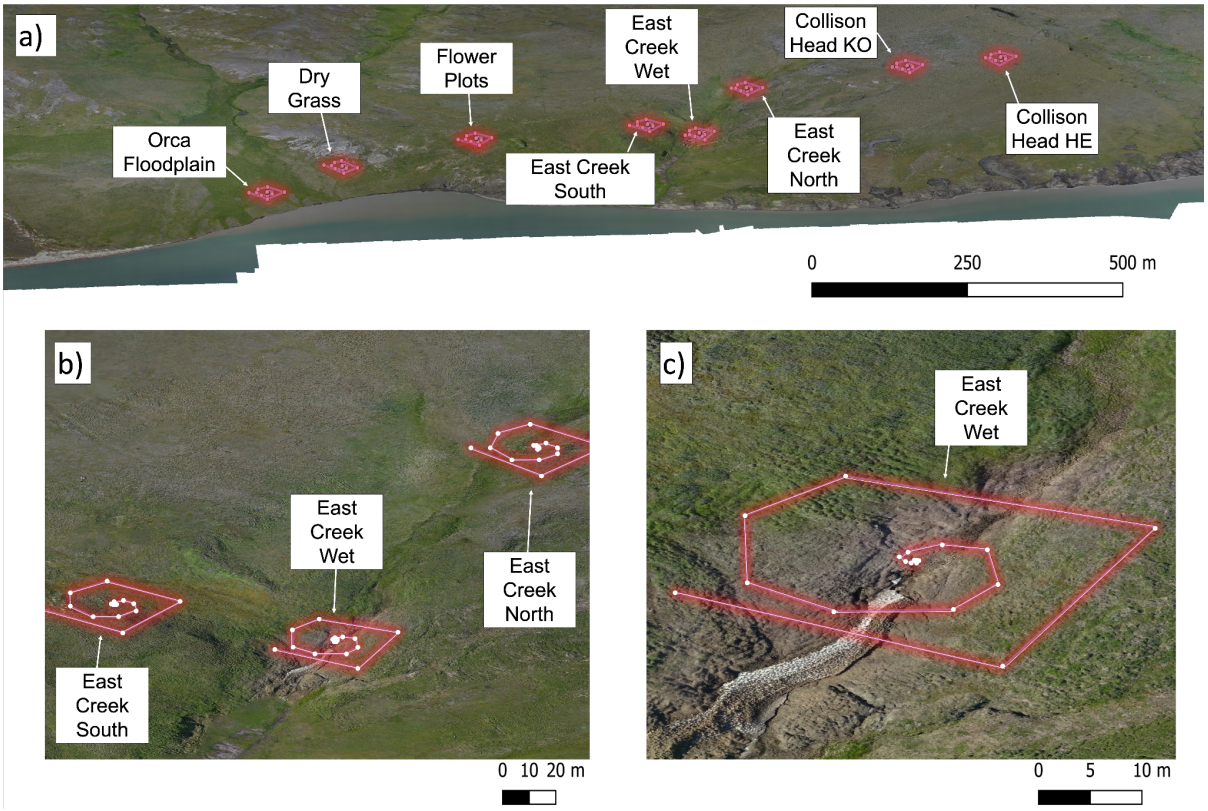

Figure 1: 20 x Green and Rooibos tea bag pairs were buried across eight spiral plots (a). The white dots (b & c) indicate the distribution of tea bag pairs within the spirals (1 x Green tea bag, 1 x Rooibos tea bag), and the red lines (a-c) represent the spiral design of each of the plots.

Tea bag Index

We used the Tea Bag Index protocol (Keuskamp et al., 2013) to investigate litter decomposition characteristics at Qikiqtaruk - Herschel Island (hereafter Qikiqtaruk) across a range of microenvironmental gradients. This protocol offers a standardised method to calculate the mass loss of specific green and rooibos tea mixes, which can be obtained globally, and allow for the protocol to be replicated across multiple biomes (Keuskamp et al., 2013). The green tea is a more labile litter with a lower carbon:nitrogen ratio than the more recalcitrant rooibos tea litter. The two tea types therefore provide a homogeneous decomposition substrate that have mass loss characteristics that correspond

well to tundra species (Thomas et al., in review), and can easily be compared to Tea Bag Index data collected globally.

Experimental design

In the summer of 2017, we buried 160 pairs of green and rooibos tea bags (320 tea bags in total) in spiral patterns to capture a range of environmental gradients and to explore similarities between samples at close vs distant proximity We established eight distinct plots along a 3 km east-west transect at Qikiqtaruk (Fig. 1). The landscape is relatively planar, with an elevation range of 72.58 m across teabag sample points, but the transect crosses a variety of soil moisture, permafrost, and vegetational gradients with differential microtopographic patterning. We planted pairs of tea bags at 2 cm depth in the soil and geolocated them using a survey grade RTK GNSS instrument accurate to ca. 3 cm. We measured the dry weight of tea bags on 11th July 2017 prior to the date of burial on 13th July 2017, and extracted the tea bags on the 9th August 2017, after 28 days left undisturbed to decompose over the course of the tundra growing season. We then dried the bags at 70°C before weighing the tea bags to establish mass loss.

Microenvironmental variables

In positioning the teabag pairs across multiple plots and in a spiral pattern, we aimed to sample different micro environmental conditions including microclimates, microtopographies, and soil properties (i.e., soil moisture content and active layer thickness). At the burial site of each of the 160 litter pairs, we recorded soil moisture and active layer thickness (observations x 160) on the 13th July when the tea bags were buried, and once again on the 9th August when the tea bag pairs were recovered. We used a Hydrosense moisture metre (Campbell Scientific, Hyde Park, NSW, Australia) to record soil moisture, and measured active layer thickness by probing the soil with a thin metal stake and measuring the vertical distance from soil surface to the top of the permafrost layer. These belowground microenvironmental variables were then matched to the correct derived microclimate and terrain estimates and tea bag index metrics for subsequent analysis.

Drone survey

We carried out topographic surveys using three drone platforms to collect RGB multispectral data at a fine (3 cm) spatial resolution: DJI Phantom 4 Pro and Advanced (multicopter), and Phantom FX-61 (fixed wing). We used photogrammetry and structure from motion with multiview steriopsis to obtain a fine-grain 10 cm spatial resolution digital surface model and orthomosaic as described in Cunliffe *et al*. (2019a, 2019b).

Microclimate and terrain estimates

We used the *microclima* package in R (Kearney et al., 2020; Maclean et al., 2019) to model surface air temperature at a 1-m spatial grain. Using our fine resolution DSM, we modelled mean surface temperatures at the study site for each day spanning the teabag burial period of 13th July to 9th August 2017. The *microclima* model incorporates local daily climate, radiation, cloud cover and coastal exposure data from gridded global datasets derived from RCNEP (Kemp et al., 2012). We summed the 28 TIF files produced through this modelling technique to produce a 28-day thermal sum variable - a metric which captures the overall heating of the ground surface over the course of the experiment. We used the precise geolocation of each tea bag pair and extracted specific topography data (elevation above sea level, slope and aspect extracted using the "starsExtra" v.0.2.7 package in R [Dorman 2021]) from the DSM. We classified the aspect of each pixel by a range into the cardinal aspects of north, south, east and west. We aggregated the DSM file from a 10 x 10 cm resolution to a 1 x 1m resolution to match the microclimate TIF, and surface temperature thermal sum (our microclimate variable) at 1 m resolution from the modelled microclimate maps.

Decomposition metrics

We calculated mass loss and decomposition characteristics following the Tea Bag Index protocol (Keuskamp et al., 2013). Using the before- and after- burial weights of the tea bags, we calculated percentage mass loss for each individual tea bag**.** Using tea bag pairs, we also calculated the stabilisation factor (*S*) for each burial point - a factor expressing the difference between the observed and the expected decomposition of tea bags. This metric indicates the amount of remaining undecomposed litter

after the period of burial, and therefore acts as a proxy for environmental inhibition to decomposition. This metric is calculated using labile green tea and was calculated as follows:

Equation 1:

$$S = 1 - (\frac{ag}{Hg})$$

$$ag = mass\ loss\ of\ green\ tea$$

$$Hg = hydrolysable\ fraction\ of\ green\ tea = 0.842$$

We also calculated the decomposition rate (*k*), a factor expressing the rate at which the decomposable fraction of litter is lost, and hence acts as a proxy for the speed of decomposition. This metric is calculated using recalcitrant rooibos tea, and was calculated as follows:

Equation 2:

$$k = ln(\frac{ar}{Mt(r) - ar})\ x\ \frac{1}{t}$$

$$ar = decomposable\ fraction\ of\ rooibos\ tea$$

$$Hr = 0.552 = hydrolysable\ fraction\ of\ rooibos\ tea$$

$$M = rooibos\ tea\ mass\ at\ time\ point\ t$$

$$ar = Hr\ x\ (1 - S)$$

$$S = stabilisation\ factor$$

Spatial statistics

To investigate the spatial patterning and scaling of both the decomposition metrics and thermal sum and the observed microenvironmental variables (soil moisture content and active layer thickness), we produced variograms using *gstat* v. 2.0-5 package in R (Pebesma, 2006). We allowed the package's algorithm to select an appropriate best fit model from the options: spherical, matern and exponential. These plots and accompanying statistics characterise any spatial autocorrelation present in the dataset, and represent varying levels of similarity between data points both within spiral plots and across the landscape.

Principal components analysis

We conducted Principal Components Analysis (PCA) using the *FactoMineR* package in R (Lê et al., 2008) to investigate spatial patterning of the modelled and observed environmental variables and decomposition metrics across the landscape. We plotted the first and second component axes to identify potential spatial patterning and clustering of our derived (thermal sum, teabag mass loss, decomposition rate, stabilisation factor) and observed variables (elevation, slope, aspect, soil moisture, active layer thickness), and to explore the extent to which any clustering was controlled by spatial patterning. Using these two forms of spatial analysis, we investigated spatial heterogeneity within the above- and below-ground conditions at the study site, and whether this heterogeneity is reflected in the spatial patterning of the decomposition metrics.

Hierarchical models

We used Bayesian linear models to run two sets of models: one set estimating soil and surface environmental controls on decomposition characteristics, and one set exploring the topographical controls (elevation, slope and aspect) of decomposition characteristics. Each of the two sets of models included a separate model featuring one of the following decomposition metrics as the response variable; green tea mass loss, rooibos tea mass loss, stabilisation factor (S) and decomposition rate (k).

For the soil and surface influences models, we fitted the model with each decomposition characteristic as the response variable, and surface temperature thermal sum, active layer thickness and soil moisture content as fixed effects. We also ran models in which we fitted the interaction between the thermal sum and active layer thickness, and the interaction between the thermal sum and soil moisture % content to investigate potential interactive effects between above- and below-ground conditions. For the topography models, we fitted the model with each of the decomposition characteristics as the response variable, and elevation, slope and aspect as fixed effects. For each of our models, we included 'plot ID' as a random effect, and did not use random slopes in our analysis due to non-convergence in each of the models.

We completed this analysis using the *brms* package (Bürkner, 2017), using weakly informative priors for all models, two chains, 8000 iterations and a warmup value of 2000. We conducted all analyses in R version 3.6.3 (R Core Team, 2013). The code and data used for this study can be downloaded here: https://github.com/ShrubHub/MicroTeaHub and https://doi.org/10.5281/zenodo.6411321. The processing reports and workflow for the drone data can be found in the respective methodologies of Cunliffe et al., 2019(a) and Cunliffe et al., 2019(b).

Results:

(1) How do microclimate, microtopography and soil conditions vary spatially across a tundra landscape?

Microclimates varied with topography across the study area

Modelled microclimate was highly variable across Qikiqtaruk. Our modelled thermal sum map represented the range of mean surface temperatures 10 cm from the surface over the burial period in summer 2017 (Fig. 2). The thermal sum across the landscape and over the study period ranged from 121-140°C. Surface temperature was negatively correlated with elevation (Pearson's -0.88, $p < 0.05$).

Predicted microclimates were coldest on north-west facing slopes and warmest in valley bottoms and south-east facing slopes.

Topography affects microclimate, but does not directly affect decomposition

We found minimal influence of elevation, slope and aspect on decomposition patterns (Fig. 2). We found no significant relationship between elevation or slope and any of the decomposition metrics (Table S1), although we acknowledge that elevation does not vary dramatically across the study site. We found a low magnitude and highly uncertain negative relationship between green tea mass loss and both elevation and slope, but no relationship between decomposition rate (k) and both elevation and slope. Contrary to our predictions, our results indicated that green tea mass loss was significantly higher (Slope 0.121, CI: 0.052-0.021) - and stabilisation factor lower (Slope: -0.095, CI: 0.041–0.174) on north-facing slopes compared to south-facing slopes (Fig. 2; Table S1).

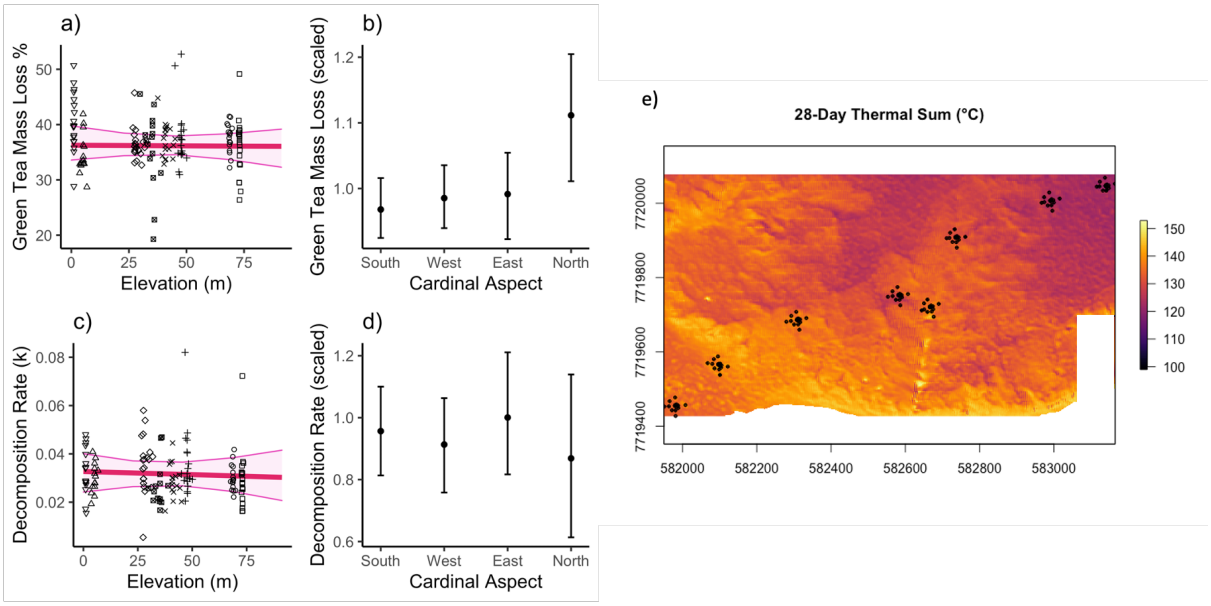

Figure 2: Green tea mass loss and decomposition rates were lower at higher elevations (a, c). Green tea mass loss was higher on north-facing slopes (b, d). The trend lines (a,c) and error bars (b,d) are Bayesian model fits with ribbons showing 95% credible intervals. Full outputs can be found in Supplementary materials (Table S1). Map of surface temperature thermal sum at 10 cm height generated using the *microclima* package (Maclean, 2020) representing conditions in July and August 2017 at Qikiqtaruk - each black dot represents a teabag burial pair (e).

Microclimates varied at larger spatial scales than soil moisture and active layer, but decomposition was highly variable across the study area

Surface temperature thermal sum varied between, but not within plots, whereas soil moisture and active layer thickness was highly heterogeneous within plots (wide range of soil moisture % within each plot) (Fig. 3). Semivariance, the degree of a correlative relationship between spatial points, of active layer thickness had a range of ~ 30 m between pixel pairs (nugget: 56.2 mm; sill: 114.8 mm), and similarly semi-variance of soil moisture content had a range of 34.7 m between pixel pairs, but did not plateau for thermal sum (Fig. 3). The unexplained spatial variability was low for the active layer thickness, soil moisture content and thermal sum models. Semi-variance did not plateau for green tea mass loss (semi-variance: 20.77%; range: 0 m). See supplementary Table 1 for variogram statistics.

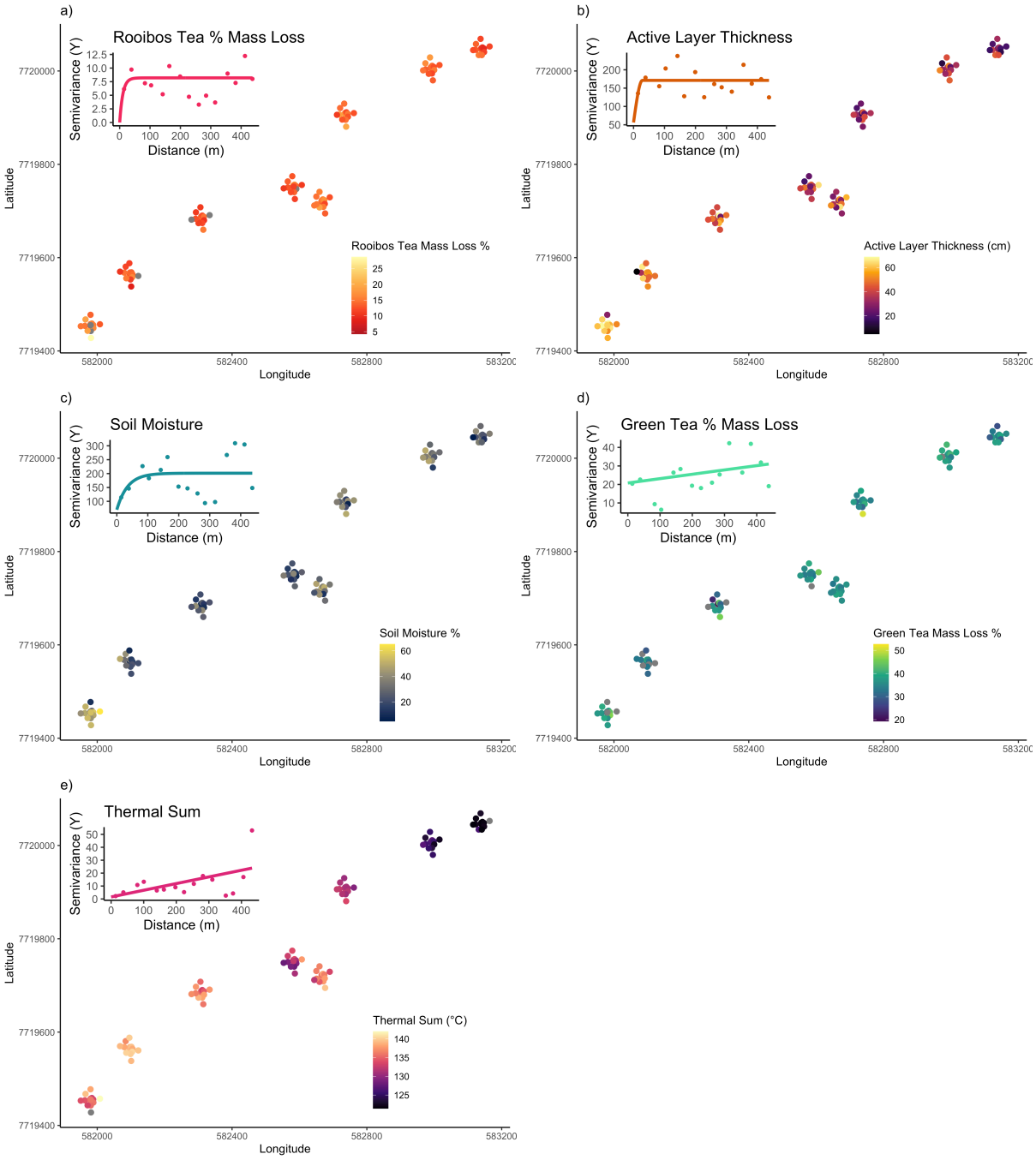

Figure 3: We found high among-plot spatial heterogeneity for rooibos tea mass loss (a), active layer thickness (b) and soil moisture % (c), in contrast to more within-splot variation in both green tea mass loss (d) and thermal sum (e). Semivariance plateaus were ~30 m for active layer thickness and < 100 m for soil moisture content, but did not plateau for surface mean temperature and green tea mass loss. Eastings and Northings are in the spatial reference system NAD83 UTM 7N (EPSG: 26907).

(2) How does microtopography, microclimate, soil moisture and active layer thickness influence litter decomposition?

416

417 ***The controls on decomposition varied across plots along the study transect***

418

419 We found significant spatial clustering of decomposition and environmental metrics on the plot-by-plot
420 scale, based on our PCA analysis. Eigenvalue analysis showed that respectively, the first three principal
421 component axes explained 28.4%, 23.2% and 17.9% of the overall variance in the data (Fig. 4). PC1
422 was more strongly associated with green tea mass loss, stabilisation factor and elevation, whereas PC2
423 was more strongly associated with thermal sum (Fig. 4). Further, while decomposition correlates best
424 with PC3, stabilisation factor correlates best with PC1. Collison Head (Komakuk vegetation
425 community) and Collison Head (Herschel vegetation community) were more strongly characterised by
426 elevation and aspect. In contrast, the Orca Floodplain plot, the wettest plot with the deepest active layer,
427 was more strongly characterised by soil moisture and active layer conditions. The Flower Plot, East
428 Creek North and East Creek South plots were more strongly associated with thermal sum and slope.
429 Overall, the microclimate variables and elevation contributed much more to the clustering of
430 observations than soil moisture content, active layer thickness, aspect and slope. These findings reflect
431 the within-plot variation of each of the observed environmental variables (Fig. 4).

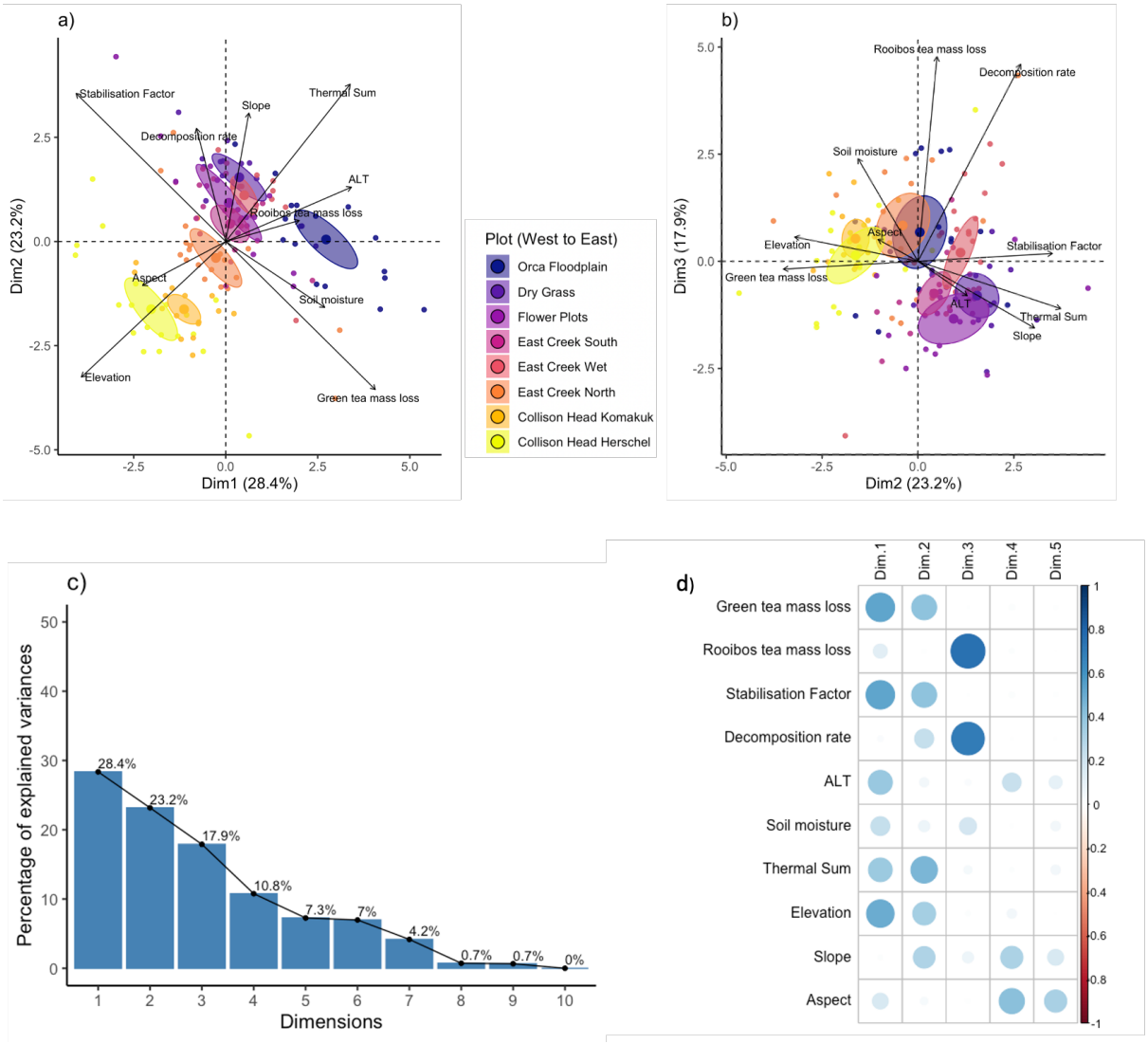

Figure 4: Plots were characterised by microclimate and elevation, while soil conditions were more spatially heterogeneous. Top panel: Principal Components Analysis (PCA) shows clustering of spiral plots by microenvironmental and decomposition variables. Microclimate and decomposition metrics contributed more to this spatial clustering than soil conditions or topography. Ellipses represent 95% confidence intervals of group clustering. Bottom Panel: mean surface temperature and elevation show low plot-specific variability, while soil moisture content and active layer thickness varies substantially within each spiral plot.

(3) Do surface microclimate and below-ground microenvironment drivers influence litter decomposition?

Soil moisture and active layer thickness influenced decomposition

We found that mass loss in labile green tea was significantly greater in wetter versus drier plots. With each increase in 10% soil moisture content, we found an additional 5.2% green tea mass loss, with a narrow margin of error (CI: -3.1 – 7.2; Fig. 5). Green tea mass loss increased to a slightly greater magnitude with higher mean surface air temperatures, though with a very wide margin of error (Slope: 3.4, CI: -20.8 – 35.9; Fig.5). The differences in soil moisture content and surface air temperature between spiral plots accounted for 22% of variance within the data. We found non-significant negative trends for the effects of these variables on the stabilisation factor (*S*) (Fig. 5, Table S1).

We also found that every increase in 10 cm active layer thickness corresponded to a 3% significant increase in green tea litter mass loss (Slope: 2.9, CI: 0.29-5.53). We found significant inverse trends for the effects of active layer thickness on green tea mass loss (Slope: -0.06, CI: -0.115--0.004). We identified no significant relationships between the environmental variables (thermal sum, soil moisture, active layer thickness), and rooibos tea mass loss or decomposition rate (*k*) (Fig. 5, Table S1).

Weak Interactions were found between temperature and soil conditions

With increasing soil moisture content and mean surface air temperatures, the stabilisation factor (*S*) decreased, indicating smaller amounts of remaining undecomposed litter after the period of burial (Fig. S1, Table S3). In contrast, we found no relationship between decomposition rate (*k*) and either soil moisture content and thermal sum. There was no strong interaction between thermal sum and active layer thickness. Our results did, however, indicate that decomposition was faster where the active layer was deeper in cooler microclimates with wetter soils, and slower in areas with deeper active layers but warmer surface temperatures and drier soils (Fig. S1, Table S3).

Controls on litter mass loss are scale dependent

The relationships between mean surface temperature, soil moisture and active layer thickness were positive on the whole-landscape (or ‘across-plots’) scale, but they varied on a plot-by-plot (or ‘within-plots’) scale (Fig. 5; Tables S1 and S2). For example, while the relationship between mean surface

473 temperature and active layer depth was only slightly positive at the landscape scale, it was strongly
474 positive at the Flower Plots. Likewise, the strongest driver of decomposition on the landscape-scale was
475 soil moisture, but the plot-scale trends differed considerably, with four plots exhibiting negative trends,
476 three plots exhibiting positive trends, and one plot exhibiting no discernable trend. These results
477 highlight not only the spatial heterogeneity of below-ground conditions across the landscape (Fig.3) but
478 also the spatial heterogeneity of the corresponding decomposition responses (Fig.5).

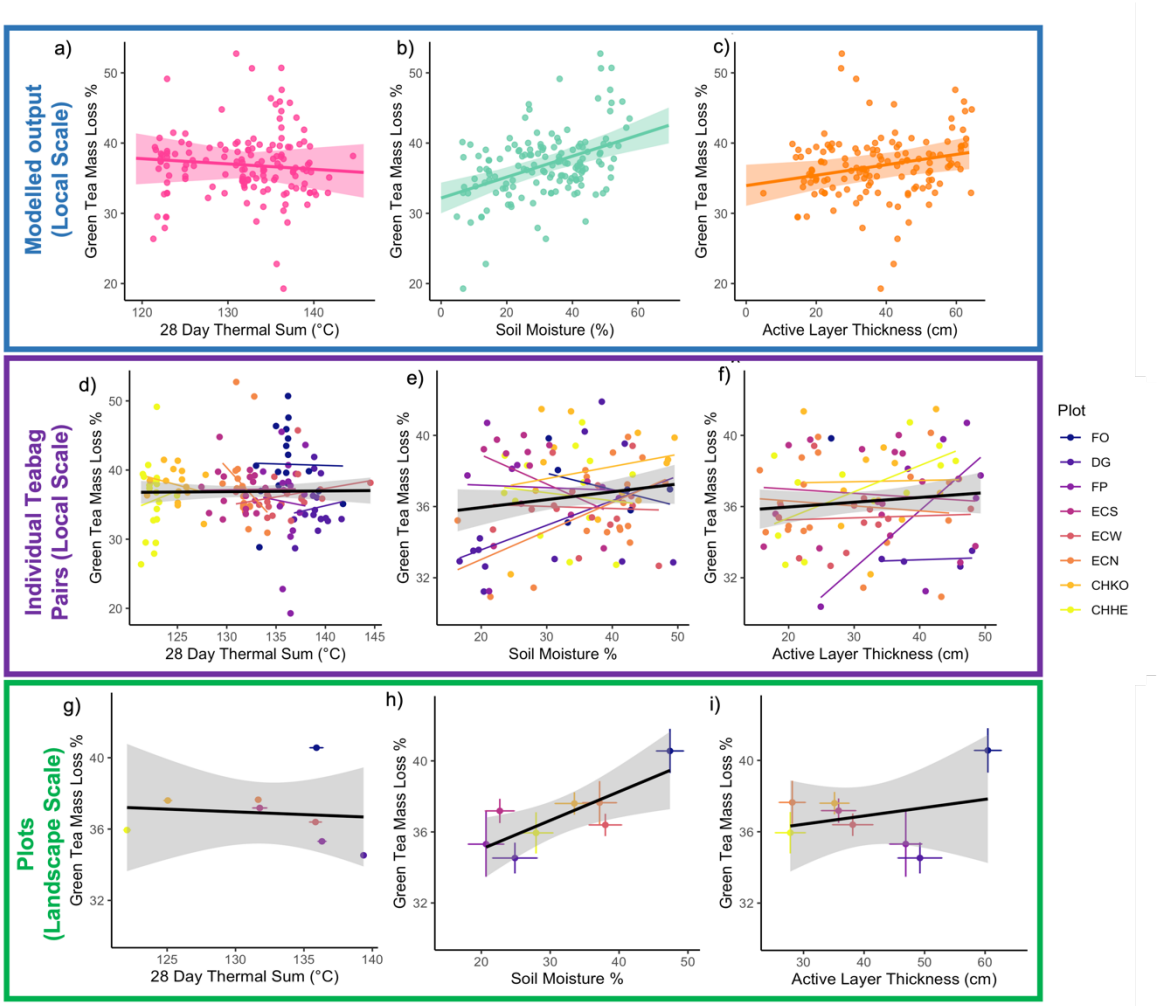

479

480 **Figure 5:** While there was a positive trend between mean surface temperature, soil moisture and active layer
481 thickness on green tea mass loss, the plot-scale trends varied considerably. For example, the relationship between
482 active layer thickness and green tea mass loss was positive at the Flower Plot plot, while the relationships between
483 both mean surface temperature and soil moisture with green tea mass loss was anomalously negative. Plots a-c
484 represent individual tea-bag pair relationships, plots d-f represent averaged plot-scale relationships. Coloured
485 trend lines (a-c) represent plot-scale trends, and grey trend lines represent landscape-scale trends (a-f). Increased

soil moisture, active layer thickness and thermal sum surface temperatures corresponded with higher green tea mass loss (g-i). The trend lines for (g-i) are Bayesian model fits with ribbons showing 95% credible intervals, while the trend lines for (a-f) are linear model fits with ribbons showing 95% confidence intervals. Full outputs can be found in Table S1.

When we ran models without the plot random effect, we found that scale dependency of these relationships - whereby some variables better explained decomposition *across* plots, while some better explained decomposition *within* plots (Table S2). For example, green tea mass loss was slightly better explained by soil moisture averaged across plots, versus within plots, although there was little difference in the within-plot versus across-plot trends for decomposition rate or stabilisation factor. Likewise, green tea mass loss was slightly better explained by active layer thickness averaged across plots, versus within plots, while decomposition rates were slightly better explained by active layer depth within plots (Table S2).

Discussion:

How do microclimate and soil conditions vary spatially across a tundra landscape?

Soil moisture and active layer depths varied more across the landscape compared to modelled temperature

Overall, we found that soil moisture and active layer thickness better explained variation in litter mass loss relative to temperatures. With each increase in 10% soil moisture content, we found an additional 5.2% green tea mass loss, with a narrow margin of error (CI: -3.1 – 7.2; Fig. 5), and with every increase in 10 cm active layer thickness corresponded to a 3% significant increase in green tea litter mass loss (Slope: 2.9, CI: 0.29-5.53), while the relationship between thermal sum and green tea mass loss was negligible. We found that variation in soil moisture and active layer thickness best explained litter mass loss within-plots (< 30 m) versus among plots across the landscape ('across plots', > 30 m, Fig. 4). Despite these scaling dependencies, the relationship between the belowground variables and

513 decomposition metrics varied considerably among plots (Fig.6; Table S1). Green tea litter mass loss
514 was greatest at 52.74% at the East Creek North plot and lowest at 19.28% at the Flower Plots site. We
515 theorise that, during peak summer season, soil moisture and active layer depth explain variation in
516 decomposition across the landscape better than surface temperature. However, at other times of year, in
517 particular during springtime soil thawing and autumn active layer thickening, temperature-permafrost
518 dynamics may have a stronger control over decomposition. Further research could help delineate the
519 seasonal dynamics of the decomposition-temperature relationship.
520
521 While modelled surface temperature appears to be an accurate predictor of decomposition on a regional
522 scale (Walker et al. [in prep]; Thomas et al. [in review]; Davidson & Janssens, 2006; Keuskamp et al.,
523 2013), it may well be the case that below-ground conditions better explain variation across finer
524 landscape scales. For example, Bradford et al. (2014) found that local plot-specific conditions explained
525 over three times the variation in global decomposition than macroclimate data. Walker et al. [in prep]
526 found evidence that soil moisture manipulations and an elevational gradient influenced decomposition
527 below and above treeline in the Southern Yukon. These findings suggest that regional macroclimate as
528 a driver of decomposition may be modulated by highly heterogeneous microenvironmental and below-
529 ground conditions (Bütikofer et al., 2020; Duffy et al., 2021). As such, Earth-system models, which use
530 coarse gridded climate data to model decomposition globally have inherently limited representations of
531 carbon cycling (Fig. 6).
532

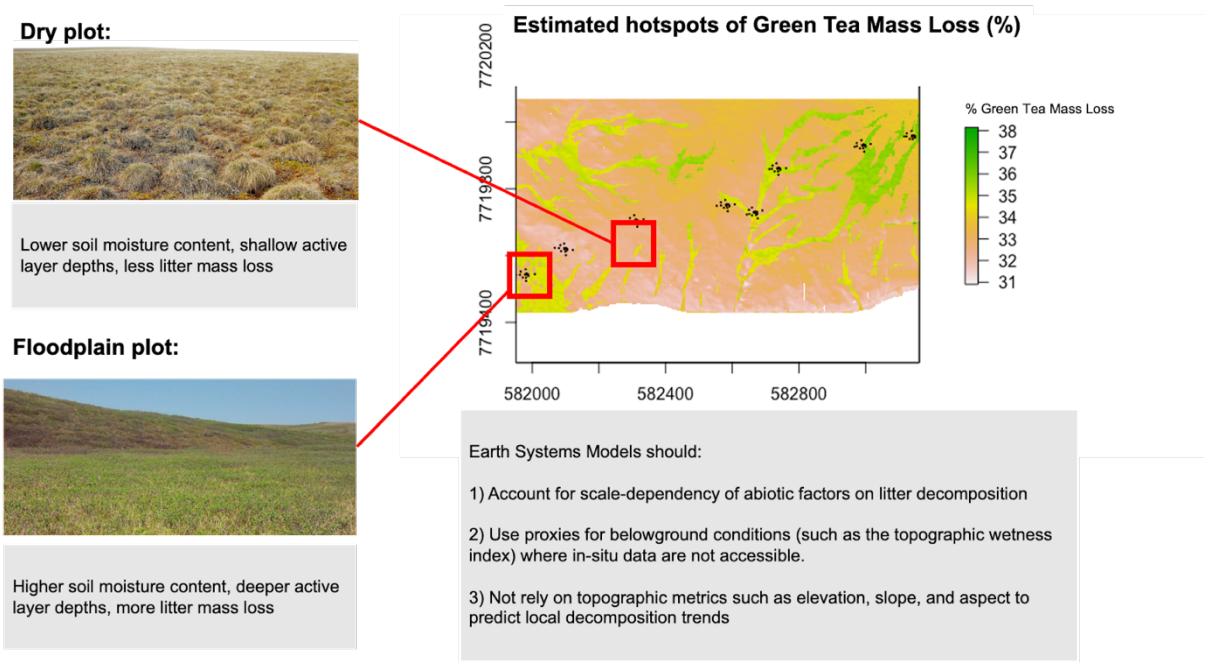

Figure 6: Map of estimated summertime green tea litter mass loss hotspots (green), using predicted slopes extracted from our Bayesian analyses (Table S1) using the microclima basemaps, and a topography wetness index map generated using the 'Dynatopmodel' package in *R* (Metcalfe et al., 2015). While decomposition patterns vary heterogeneously across microclimates, we expect to observe greater decomposition in 'floodplain' environments following natural drainage. Black points represent tea-bag pairs within spiral plots. We list recommendations for Earth-system modellers based on our findings.

How does microtopography, microclimate, soil moisture and active layer thickness influence litter decomposition?

Decomposition was poorly explained by variation in topography and aspect

On Qikiqtaruk, where we conducted our study, belowground microenvironmental effects appear to outweigh the temperature and topography effects on decomposition. We initially predicted that decomposition would decrease with elevation due to warmer microclimates, more optimal drainage and reduced exposure. We found slight decreases in mass loss with increasing elevation in our data, but also slightly greater decomposition on north-facing slopes (Fig. 2). It should be noted that the study has undulating terrain, so is not entirely comparable with studies investigating the links between elevation,

552 slope and aspect and decomposition. In alpine tundra, studies often find that mass loss decreases with
553 increased altitude, corresponding with lower soil temperatures at higher altitudes (Speed et al., 2015;
554 Sveinbjörnsson et al., 1995). However, other studies have reported faster decomposition rates with
555 increasing elevations, corresponding with moister soils at high elevations (Walker et al., [in prep];
556 (Murphy et al., 1998). Overall, elevation was not a major driver of decomposition at Qikiqtaruk.
557
558 ***Soil moisture rather than surface temperature controlled decomposition across the landscape***
559 We observed greater mass loss and faster decomposition rates in wetter areas, and to a lesser extent
560 areas with deeper active layers, across the landscape on Qikiqtaruk (Fig. 5). Many studies report air
561 temperature as the primary control of decomposition rates, both globally and in tundra ecosystems (e.g.
562 Hobbie, 1996; Sierra et al., 2015). However, we found that green tea mass loss at Qikiqtaruk was more
563 sensitive to soil moisture content, suggesting soil moisture conditions may actually be a better predictor
564 of litter decomposition in the Arctic tundra (Thomas et al. [in review], Walker et al. [in prep]; Aerts,
565 2006; Hicks Pries et al., 2013; Murphy et al., 1998). Soil moisture content may be the major limiting
566 factor of decomposition in Arctic tundra ecosystems because wetter soils promote enhanced microbial
567 and detritivore activity (Aerts, 2006; Murphy et al., 1998; Rinnan et al., 2008; Swift et al., 1979; Thakur
568 et al., 2018; Waring & Schlesinger, 1985). Where waterlogged soils create anoxic belowground
569 conditions, we may expect to see reduced decomposition (Davidson & Janssens, 2006), although the
570 soil moisture measured in our study did not exceed the saturation threshold at most tea bag locations.
571 In the case of Qikiqtaruk, soil moisture had a range of 60.4% suggesting highly heterogeneous
572 decomposition trends across the landscape driven, at least in part, by variable soil moisture conditions.
573 Our findings support previous studies highlighting the importance of soil moisture as a control over
574 decomposition in tundra ecosystems.
575
576 **Do surface microclimate and below-ground microenvironment drivers interact to**
577 **influence litter decomposition?**
578

Interactive effects among microenvironment and temperature on decomposition were weak

Although we did observe consistently greater mass loss in wetter plots with deeper active layers, interaction effects were weak (Fig. S1; Table S3). Our results support the idea that large-scale variation in litter decomposition can be explained by climate (Davidson & Janssens, 2006; Keuskamp et al., 2013; Swift et al., 1979; Waring & Schlesinger, 1985), but suggest that at the landscape-scale variation in microenvironmental conditions such as soil moisture and active layer play a greater role. Soil moisture, active layer thaw depths and surface temperature should be considered in the modelling of future decomposition trends, because warmer summers may contribute to drought conditions and increased drainage in tundra soils due to thaw (Hicks Pries et al., 2013). This feedback response may be further complicated by a predicted increase in precipitation in northern latitudes (Sierra et al., 2015). Our study did not investigate the presence of soil fauna or microbial activity, but there is evidence to suggest that soil fauna presence (which increases litter decomposition) is globally driven by both soil moisture content (García-Palacios et al., 2013; Thakur et al., 2018) and global temperature patterns (Wall et al., 2008). We did however, observe fungal biomass in soils during the extraction of our tea bags at some plots, suggesting that the below-ground biotic environment could be an important factor explaining litter decomposition across this study system. Future decomposition studies should investigate the importance of below-ground heterogeneity in soil fauna presence, microbial and fungal activity and diversity of the below-ground community on decomposition across the tundra.

Active layer depth altered decomposition-temperature relationships

We found limited influence of active layer thickness alone on decomposition characteristics (Table S1; Fig. 5). Although the interactive effects between microclimate and active layer thickness were not statistically significant, we found that the decomposition – temperature relationship was positive for deeper active layers and negative for shallower active layers. Decomposition rates were slower in areas with deeper active layers and warmer surface microclimates, but faster in areas with deeper active layers but colder surface microclimates. Conversely, decomposition rates were faster in areas with shallow active layers and warmer surface microclimates, but slower in areas with shallow active layers and colder surface microclimates. This finding contradicts the hypothesis that warming soils (with

607 deepening active layers) will promote faster decomposition and therefore enhance carbon losses. Active
608 layer depth was weakly correlated with soil moisture, so part of this effect could be attributable in part
609 to soil moisture variation among different plots across the study plot. The process of climate warming
610 and the subsequent thawing of permafrost has previously been shown to increase the rate of microbial-
611 driven decomposition and the exposure of these microbes to substantial quantities of ancient buried
612 carbon (Nowinski et al., 2010; Xue et al., 2016). However, our experimental test of near-surface
613 decomposition may demonstrate the influence of active layer depths on surface soil conditions including
614 soil temperature and moisture. These potential interactive effects between shallow versus deep active
615 layers and near-surface soil conditions on decomposition rates complicates our ability to predict carbon
616 cycling based solely on permafrost dynamics or air temperatures.
617
618 ***Decomposition is likely influenced by the lability of litter inputs across tundra landscapes***
619 Litter type, and thus quality, is widely considered to be one of the most important predictors of
620 decomposition (Bradford et al., 2014; Cornwell et al., 2008; Hobbie, 1996; Sundqvist et al., 2011). We
621 found greater mass loss for labile green tea relative to recalcitrant rooibos tea bags, both of which show
622 similar decomposition characteristics to plant species common in Arctic tundra landscapes (Thomas et
623 al., [in prep]). Vegetation change is widespread across tundra ecosystems, particularly as shrub
624 communities, with generally more recalcitrant woody litter, are becoming more dominant (Elmendorf
625 et al., 2012a; Myers-Smith, Forbes, et al., 2011). These widespread 'shrubification' trends may lead to
626 a biome-wide negative feedback response whereby more recalcitrant shrub litter becomes increasingly
627 dominant and moderates carbon cycling (Cornelissen et al., 2007), although these vegetation shifts may
628 lag somewhat behind climatic change (Bjorkman et al., 2018). However, many tundra species produce
629 abundant leaf litter that is quite labile (Cornelissen et al., 2007b; Shaver et al., 2006), and graminoid
630 and other vegetation types are increasing in many tundra ecosystems (Elmendorf et al. 2012). Thus, the
631 direction of vegetation-decomposition feedbacks with warming remain unclear.
632
633 ***Future decomposition in tundra ecosystems will be influenced by vegetation change***

Our results demonstrate differential decomposition rates between litter types, an observation which supports the idea that future vegetation change will impact litter mass loss dynamics in a warming Arctic. Vegetation community responses to climate warming are highly variable among vegetation communities and tundra plots (Myers-Smith et al., 2020; Elmendorf et al., 2012b), and as such the composition of plant litter will likely also shift in a spatially heterogeneous way. We may expect to see local-scale shifts in plant community composition driven strongly by microenvironmental variation such as for example snow melt, soil moisture and soil temperatures (Niittynen et al., 2020). Changing vegetation patterns may also lead to further plant-driven microenvironmental changes, such as shifts in localised surface albedo (Sturm et al., 2005), or snow-trapping from taller shrubs (DeMarco et al., 2014). We also expect future tundra vegetation community change along elevational gradients (Myers-Smith, Forbes, et al., 2011), which may indirectly induce changes in litter decomposition rates due to decomposition being strongly sensitive to litter quality (e.g. Aerts, 2006; Buckeridge et al., 2010; Hobbie, 1996). While we have shown decomposition to be sensitive to belowground microenvironments, projections of future tundra carbon cycling must also account for potential vegetation community change across scales.

There is a fundamental mismatch between macro-scale predictions of biological processes based on gridded datasets, and micro-scale predictions based on high-resolution site specific observations (Bütikofer et al., 2020). The magnitude and direction of carbon cycling trends in the Arctic are contingent not only on climate warming and future precipitation trends, but also on future vegetation change. Tundra vegetation change is strongly controlled by local abiotic factors (Chapin et al., 2005; Elmendorf et al., 2012a; Myers-Smith, Forbes, et al., 2011; Myers-Smith & Hik, 2018). Our results show that litter mass loss was more strongly controlled by heterogeneous microenvironmental factors such as soil moisture content. The discrepancy between macro and micro-scale predictions may account for variability in the modelling of soil CO_2 emissions and the estimation of current carbon stocks within the tundra (De Deyn et al., 2008; Del Grosso et al., 2005; Sierra et al., 2015). We acknowledge that biome-scale, and global-scale carbon cycling models cannot incorporate the fine-grain resolution that we can explore in site-specific studies. However, we call for more consideration of scale-dependency

when predicting future carbon storage and losses, for example including meso-scale estimates of soil moisture conditions into earth systems models, or adding uncertainty to models to account for spatial variability, and process uncertainty relating to above-belowground feedbacks.

Conclusion

In this study, we found that litter mass loss was greater in areas with greater soil moisture content, deeper active layer, and broadly in areas with warmer microclimates. Additionally, we found that elevation, slope and aspect were not accurate predictors of decomposition metrics at our study site. Notably, we found that the environmental controls on decomposition were highly scale dependent. We found that belowground conditions better explain variation in decomposition than temperature at the landscape-scale (> 30 m). Earth-system models predict future carbon cycling through the use of coarse gridded climate datasets and a mechanistic understanding of macro-scale correlations between environmental drivers and tundra decomposition rates (Carey et al., 2016; Crowther et al., 2016; Van Gestel et al., 2018). Our study has highlighted that heterogeneous microenvironmental conditions in the Arctic tundra influence decomposition. As such, we argue that the predictive power of biome-wide carbon cycling estimates are compromised by a strong macroclimate focus. Capturing and accounting for scale-dependency of ecological processes such as decomposition with climate change remains a major and timely challenge for the field of global change ecology.

690 **Code and data availability:**

691 The study was pre-registered here: https://osf.io/r3824/. The code and data used for this study can be
692 downloaded here: https://github.com/ShrubHub/MicroTeaHub. For access to, and use of the large
693 DSM and thermal sum TIFF files, which are too large to store in the repository, see:
694 https://doi.org/10.5281/zenodo.6411321.
695
696 **Author contributions:**

697 JK conceived of the study with inputs from IMS, and the experimental design was conceived by both
698 GND and IMS. AC collected and processed the drone data, and the ground field data collection was
699 completed by GND and IMS. HT completed initial data processing. HT and GND processed the tea
700 bags after extraction from the ground. Funding was acquired by IMS, EG and JK. All data cleaning,
701 statistical analyses and writing were completed by EG, with editorial input from GND, IMS, JK, HT
702 and AC.
703
704 **Acknowledgements:**

705 We wish to thank the Qikiqtaruk Territorial Park staff including Richard Gordon, Edward McLeod,
706 Samuel McLeod, Ricky Joe, and Shane Goesen, as well as the Yukon government and Yukon parks for
707 their permission and support of this research (permit number Inu0216). We also thank the Inuvialuit
708 people for their permission to work on their traditional lands, and William Palmer for assistance with
709 the UAV surveys.
710
711 **Financial support:**

712 This research was supported by the Natural Environment Research Council (grant NE/M016323/1 to
713 IMS; grant NE/S007407/1 to EG), the National Geographic Society (grant CP-061R-17 to JK), and the
714 NERC Geophysical Equipment Facility (grants GEF:1063 and GEF:1069 to IMS and AC).
715
716 **Conflict of Interest statement:**

717 The authors have no conflicts of interest to declare.
718
719
720
721
722
723
724

References:

Ackerman, D., Griffin, D., Hobbie, S. E., & Finlay, J. C. (2017). Arctic shrub growth trajectories differ across soil moisture levels. *Global Change Biology*, *23*(10), 4294–4302. https://doi.org/10.1111/gcb.13677

Aerts, R. (2006). The freezer defrosting: Global warming and litter decomposition rates in cold biomes. *Journal of Ecology*, *94*(4), 713–724.

Aerts, R., Callaghan, T. V., Dorrepaal, E., Van Logtestijn, R. S. P., & Cornelissen, J. H. C. (2012). Seasonal climate manipulations have only minor effects on litter decomposition rates and N dynamics but strong effects on litter P dynamics of sub-arctic bog species. *Oecologia*, *170*(3), 809–819.

Aguirre, D., Benhumea, A. E., & McLaren, J. R. (2021). Shrub encroachment affects tundra ecosystem properties through their living canopy rather than increased litter inputs. *Soil Biology and Biochemistry*, *153*, 108121. https://doi.org/10.1016/j.soilbio.2020.108121

AMAP, 2021. Arctic Climate Change Update 2021: Key Trends and Impacts. Summary for Policy-makers. Arctic Monitoring and Assessment Programme (AMAP), Tromsø, Norway. 16 pp

Assmann, J. J., Myers-Smith, I. H., Kerby, J. T., Cunliffe, A. M., & Daskalova, G. N. (2020). Drone data reveal heterogeneity in tundra greenness and phenology not captured by satellites. *Environmental Research Letters*, *15*(12), 125002.

Berner, L. T., Massey, R., Jantz, P., Forbes, B. C., Macias-Fauria, M., Myers-Smith, I., Kumpula, T., Gauthier, G., Andreu-Hayles, L., Gaglioti, B. V., Burns, P., Zetterberg, P., D'Arrigo, R., & Goetz, S. J. (2020). Summer warming explains widespread but not uniform greening in the Arctic tundra biome. *Nature Communications*, *11*(1), 4621. https://doi.org/10.1038/s41467-020-18479-5

Bintanja, R., & Andry, O. (2017). Towards a rain-dominated Arctic. *Nature Climate Change*, *7*(4), 263–267. https://doi.org/10.1038/nclimate3240

Bjorkman, A. D., Myers-Smith, I. H., Elmendorf, S. C., Normand, S., Rüger, N., Beck, P. S., Blach-Overgaard, A., Blok, D., Cornelissen, J. H. C., & Forbes, B. C. (2018). Plant functional trait change across a warming tundra biome. *Nature*, *562*(7725), 57–62.

Björnsdóttir, K., Barrio, I. C., & Jónsdóttir, I. S. (2021). Long-term warming manipulations reveal complex decomposition responses across different tundra vegetation types. *Arctic Science*, *ja*.

Blume-Werry, G., Di Maurizio, V., Beil, I., Lett, S., Schwieger, S., & Kreyling, J. (2021). Don't drink it, bury it: Comparing decomposition rates with the tea bag index is possible without prior leaching. *Plant and Soil*, 1–9.

Bond-Lamberty, B., & Thomson, A. (2010). Temperature-associated increases in the global soil respiration record. *Nature*, *464*(7288), 579–582.

Bradford, M. A., Warren II, R. J., Baldrian, P., Crowther, T. W., Maynard, D. S., Oldfield, E. E., Wieder, W. R., Wood, S. A., & King, J. R. (2014). Climate fails to predict wood decomposition at regional scales. *Nature Climate Change*, *4*(7), 625–630.

Buckeridge, K. M., Zufelt, E., Chu, H., & Grogan, P. (2010). Soil nitrogen cycling rates in low arctic shrub tundra are enhanced by litter feedbacks. *Plant and Soil*, *330*(1–2), 407–421.

Bürkner, P.-C. (2017). brms: An R package for Bayesian multilevel models using Stan. *Journal of Statistical Software*, *80*(1), 1–28.

Burn, C. R., & Zhang, Y. (2009). Permafrost and climate change at Herschel Island (Qikiqtaruq), Yukon Territory, Canada. *Journal of Geophysical Research: Earth Surface*, *114*(F2).

Bütikofer, L., Anderson, K., Bebber, D. P., Bennie, J. J., Early, R. I., & Maclean, I. M. (2020). The problem of scale in predicting biological responses to climate. *Global Change Biology*, *26*(12), 6657–6666.

Carey, J. C., Tang, J., Templer, P. H., Kroeger, K. D., Crowther, T. W., Burton, A. J., Dukes, J. S., Emmett, B., Frey, S. D., & Heskel, M. A. (2016). Temperature response of soil respiration largely unaltered with experimental warming. *Proceedings of the National Academy of Sciences*, *113*(48), 13797–13802.

Change, I. C. (2013). The Physical Science Basis. 2013. *Intergovernmental Panel On Climate Change AR4 WG1*.

780 Chapin, F. S., Sturm, M., Serreze, M. C., McFadden, J. P., Key, J. R., Lloyd, A. H., McGuire, A. D.,
781 Rupp, T. S., Lynch, A. H., & Schimel, J. P. (2005). Role of land-surface changes in Arctic
782 summer warming. *Science*, *310*(5748), 657–660.
783 Cornelissen, J. H., Van Bodegom, P. M., Aerts, R., Callaghan, T. V., Van Logtestijn, R. S., Alatalo,
784 J., Stuart Chapin, F., Gerdol, R., Gudmundsson, J., & Gwynn-Jones, D. (2007a). Global
785 negative vegetation feedback to climate warming responses of leaf litter decomposition rates
786 in cold biomes. *Ecology Letters*, *10*(7), 619–627.
787 Cornelissen, J. H., Van Bodegom, P. M., Aerts, R., Callaghan, T. V., Van Logtestijn, R. S., Alatalo,
788 J., Stuart Chapin, F., Gerdol, R., Gudmundsson, J., & Gwynn-Jones, D. (2007b). Global
789 negative vegetation feedback to climate warming responses of leaf litter decomposition rates
790 in cold biomes. *Ecology Letters*, *10*(7), 619–627.
791 Cornwell, W. K., Cornelissen, J. H., Amatangelo, K., Dorrepaal, E., Eviner, V. T., Godoy, O.,
792 Hobbie, S. E., Hoorens, B., Kurokawa, H., & Pérez-Harguindeguy, N. (2008). Plant species
793 traits are the predominant control on litter decomposition rates within biomes worldwide.
794 *Ecology Letters*, *11*(10), 1065–1071.
795 Crowther, T. W., Todd-Brown, K. E., Rowe, C. W., Wieder, W. R., Carey, J. C., Machmuller, M. B.,
796 Snoek, B. L., Fang, S., Zhou, G., & Allison, S. D. (2016). Quantifying global soil carbon
797 losses in response to warming. *Nature*, *540*(7631), 104–108.
798 Cunliffe, A., I. Myers-Smith. J. Kerby and W. Palmer (2019a). Orthomosaic of permafrost
799 landscape on Qikiqtaruk – Herschel Island, Yukon, Canada: August 2017. NERC Polar Data
800 Centre. DOI:10.5285/29bf1c9f-a39a-452c-b9f9-de35d9fb9179.
801 Cunliffe, A., G. Tanski, B. Radosavljevic, W. Palmer, T. Sachs, H. Lantuit, J. Kerby, and I.
802 Myers-Smith (2019b) Rapid retreat of permafrost coastline observed with aerial drone
803 photogrammetry. The Cryosphere 13(5):1513-1528. DOI: 10.5194/tc-13-1513-2019.
804 Davidson, E. A., & Janssens, I. A. (2006). Temperature sensitivity of soil carbon decomposition and
805 feedbacks to climate change. *Nature*, *440*(7081), 165–173.
806 De Deyn, G. B., Cornelissen, J. H., & Bardgett, R. D. (2008). Plant functional traits and soil carbon
807 sequestration in contrasting biomes. *Ecology Letters*, *11*(5), 516–531.
808 Del Grosso, S. J., Parton, W. J., Mosier, A. R., Holland, E. A., Pendall, E., Schimel, D. S., & Ojima,
809 D. S. (2005). Modeling soil CO 2 emissions from ecosystems. *Biogeochemistry*, *73*(1), 71–91.
810 DeMarco, J., Mack, M. C., & Bret-Harte, M. S. (2014). Effects of arctic shrub expansion on
811 biophysical vs. Biogeochemical drivers of litter decomposition. *Ecology*, *95*(7), 1861–1875.
812 Dorman, M. (2021). starsExtra: Miscellaneous Functions for Working with 'stars' Rasters. R
813 package version 0.2.7. https://CRAN.R-project.org/package=starsExtra
814 Duffy, J. P., Anderson, K., Fawcett, D., Curtis, R. J., & Maclean, I. M. D. (2021). Drones provide
815 spatial and volumetric data to deliver new insights into microclimate modelling. *Landscape*
816 *Ecology*, *36*(3), 685–702. https://doi.org/10.1007/s10980-020-01180-9
817 Elmendorf, S. C., Henry, G. H., Hollister, R. D., Björk, R. G., Bjorkman, A. D., Callaghan, T. V.,
818 Collier, L. S., Cooper, E. J., Cornelissen, J. H., & Day, T. A. (2012). Global assessment of
819 experimental climate warming on tundra vegetation: Heterogeneity over space and time.
820 *Ecology Letters*, *15*(2), 164–175.
821 Elmendorf, S. C., Henry, G. H., Hollister, R. D., Björk, R. G., Boulanger-Lapointe, N., Cooper, E. J.,
822 Cornelissen, J. H., Day, T. A., Dorrepaal, E., & Elumeeva, T. G. (2012). Plot-scale evidence
823 of tundra vegetation change and links to recent summer warming. *Nature Climate Change*,
824 *2*(6), 453–457.
825 García-Palacios, P., Maestre, F. T., Kattge, J., & Wall, D. H. (2013). Climate and litter quality
826 differently modulate the effects of soil fauna on litter decomposition across biomes. *Ecology*
827 *Letters*, *16*(8), 1045–1053.
828 Hicks Pries, C. E., Schuur, E. A. G., Vogel, J. G., & Natali, S. M. (2013). Moisture drives surface
829 decomposition in thawing tundra. *Journal of Geophysical Research: Biogeosciences*, *118*(3),
830 1133–1143.
831 Hobbie, S. E. (1996). Temperature and plant species control over litter decomposition in Alaskan
832 tundra. *Ecological Monographs*, *66*(4), 503–522.
833 Hobbie, S. E., Schimel, J. P., Trumbore, S. E., & Randerson, J. R. (2000). Controls over carbon
834 storage and turnover in high-latitude soils. *Global Change Biology*, *6*(S1), 196–210.

https://doi.org/10.1046/j.1365-2486.2000.06021.x

Holtmeier, F.-K., & Broll, G. (2005). Sensitivity and response of northern hemisphere altitudinal and polar treelines to environmental change at landscape and local scales. *Global Ecology and Biogeography*, *14*(5), 395–410. https://doi.org/10.1111/j.1466-822X.2005.00168.x

Hugelius, G., Strauss, J., Zubrzycki, S., Harden, J. W., Schuur, E. A. G., Ping, C.-L., Schirrmeister, L., Grosse, G., Michaelson, G. J., & Koven, C. D. (2014). Estimated stocks of circumpolar permafrost carbon with quantified uncertainty ranges and identified data gaps. *Biogeosciences (Online)*, *11*(23).

IPCC, 2021: Climate Change 2021: The Physical Science Basis. Contribution of Working Group I to the Sixth Assessment Report of the Intergovernmental Panel on Climate Change [Masson-Delmotte, V., P. Zhai, A. Pirani, S.L. Connors, C. Péan, S. Berger, N. Caud, Y. Chen, L. Goldfarb, M.I. Gomis, M. Huang, K. Leitzell, E. Lonnoy, J.B.R. Matthews, T.K. Maycock, T. Waterfield, O. Yelekçi, R. Yu, and B. Zhou (eds.)]. Cambridge University Press. In Press.

Kaufman, D. S., Schneider, D. P., McKay, N. P., Ammann, C. M., Bradley, R. S., Briffa, K. R., Miller, G. H., Otto-Bliesner, B. L., Overpeck, J. T., & Vinther, B. M. (2009). Recent warming reverses long-term Arctic cooling. *Science*, *325*(5945), 1236–1239.

Kemp, M. U., Loon, E. E. van, Shamoun-Baranes, J., & Bouten, W. (2012). RNCEP: Global weather and climate data at your fingertips. *Methods in Ecology and Evolution*, *3*(1), 65–70. https://doi.org/10.1111/j.2041-210X.2011.00138.x

Kemppinen, J., Niittynen, P., le Roux, P. C., Momberg, M., Happonen, K., Aalto, J., Rautakoski, H., Enquist, B. J., Vandvik, V., Halbritter, A. H., Maitner, B., & Luoto, M. (2021). Consistent trait–environment relationships within and across tundra plant communities. *Nature Ecology & Evolution*, *5*(4), 458–467. https://doi.org/10.1038/s41559-021-01396-1

Kemppinen, J., Niittynen, P., Virkkala, A.-M., Happonen, K., Riihimäki, H., Aalto, J., & Luoto, M. (2021). Dwarf Shrubs Impact Tundra Soils: Drier, Colder, and Less Organic Carbon. *Ecosystems*, *24*(6), 1378–1392. https://doi.org/10.1007/s10021-020-00589-2

Keuskamp, J. A., Dingemans, B. J., Lehtinen, T., Sarneel, J. M., & Hefting, M. M. (2013). Tea Bag Index: A novel approach to collect uniform decomposition data across ecosystems. *Methods in Ecology and Evolution*, *4*(11), 1070–1075.

Lembrechts, J. J., Hoogen, J., Aalto, J., Ashcroft, M. B., De Frenne, P., Kemppinen, J., Kopecký, M., Luoto, M., Maclean, I. M. D., Crowther, T. W., Bailey, J. J., Haesen, S., Klinges, D. H., Niittynen, P., Scheffers, B. R., Van Meerbeek, K., Aartsma, P., Abdalaze, O., Abedi, M., … Lenoir, J. (2022). Global maps of soil temperature. *Global Change Biology*. https://eprints.whiterose.ac.uk/183991/

Lembrechts, J. J., & Nijs, I. (2020). Microclimate shifts in a dynamic world. *Science*. https://doi.org/10.1126/science.abc1245

Maclean, I. M. (2020). Predicting future climate at high spatial and temporal resolution. *Global Change Biology*, *26*(2), 1003–1011.

Mekonnen, Z. A., Riley, W. J., Berner, L. T., Bouskill, N. J., Torn, M. S., Iwahana, G., Breen, A. L., Myers-Smith, I. H., Criado, M. G., Liu, Y., Euskirchen, E. S., Goetz, S. J., Mack, M. C., & Grant, R. F. (2021). Arctic tundra shrubification: A review of mechanisms and impacts on ecosystem carbon balance. *Environmental Research Letters*, *16*(5), 053001. https://doi.org/10.1088/1748-9326/abf28b

Metcalfe, P., Beven, K., & Freer, J. (2015). Dynamic TOPMODEL: A new implementation in R and its sensitivity to time and space steps. *Environmental Modelling & Software*, *72*, 155–172. https://doi.org/10.1016/j.envsoft.2015.06.010

Miner, K. R., Turetsky, M. R., Malina, E., Bartsch, A., Tamminen, J., McGuire, A. D., Fix, A., Sweeney, C., Elder, C. D., & Miller, C. E. (2022). Permafrost carbon emissions in a changing Arctic. *Nature Reviews Earth & Environment*, *3*(1), 55–67. https://doi.org/10.1038/s43017-021-00230-3

Monitoring, A. (2017). *Snow, Water, Ice and Permafrost in the Arctic (SWIPA); Summary for Policy-makers*.

Murphy, K. L., Klopatek, J. M., & Klopatek, C. C. (1998). The effects of litter quality and climate on decomposition along an elevational gradient. *Ecological Applications*, *8*(4), 1061–1071.

Myers-Smith, I. H., Elmendorf, S. C., Beck, P. S., Wilmking, M., Hallinger, M., Blok, D., Tape, K. D., Rayback, S. A., Macias-Fauria, M., & Forbes, B. C. (2015). Climate sensitivity of shrub growth across the tundra biome. *Nature Climate Change*, *5*(9), 887–891.

Myers-Smith, I. H., Forbes, B. C., Wilmking, M., Hallinger, M., Lantz, T., Blok, D., Tape, K. D., Macias-Fauria, M., Sass-Klaassen, U., & Lévesque, E. (2011). Shrub expansion in tundra ecosystems: Dynamics, impacts and research priorities. *Environmental Research Letters*, *6*(4), 045509.

Myers-Smith, I. H., Grabowski, M. M., Thomas, H. J. D., Angers-Blondin, S., Daskalova, G. N., Bjorkman, A. D., Cunliffe, A. M., Assmann, J. J., Boyle, J. S., McLeod, E., McLeod, S., Joe, R., Lennie, P., Arey, D., Gordon, R. R., & Eckert, C. D. (2019). Eighteen years of ecological monitoring reveals multiple lines of evidence for tundra vegetation change. *Ecological Monographs*, *89*(2), e01351. https://doi.org/10.1002/ecm.1351

Myers-Smith, I. H., & Hik, D. S. (2013). Shrub canopies influence soil temperatures but not nutrient dynamics: An experimental test of tundra snow–shrub interactions. *Ecology and Evolution*, *3*(11), 3683–3700.

Myers-Smith, I. H., & Hik, D. S. (2018). Climate warming as a driver of tundra shrubline advance. *Journal of Ecology*, *106*(2), 547–560.

Myers-Smith, I. H., Hik, D. S., Kennedy, C., Cooley, D., Johnstone, J. F., Kenney, A. J., & Krebs, C. J. (2011). Expansion of Canopy-Forming Willows Over the Twentieth Century on Herschel Island, Yukon Territory, Canada. *Ambio*, *40*(6), 610–623. https://doi.org/10.1007/s13280-011-0168-y

Myers-Smith, I. H., Kerby, J. T., Phoenix, G. K., Bjerke, J. W., Epstein, H. E., Assmann, J. J., John, C., Andreu-Hayles, L., Angers-Blondin, S., Beck, P. S. A., Berner, L. T., Bhatt, U. S., Bjorkman, A. D., Blok, D., Bryn, A., Christiansen, C. T., Cornelissen, J. H. C., Cunliffe, A. M., Elmendorf, S. C., … Wipf, S. (2020). Complexity revealed in the greening of the Arctic. *Nature Climate Change*, *10*(2), 106–117. https://doi.org/10.1038/s41558-019-0688-1

Niittynen, P., Heikkinen, R. K., Aalto, J., Guisan, A., Kemppinen, J., & Luoto, M. (2020). Fine-scale tundra vegetation patterns are strongly related to winter thermal conditions. *Nature Climate Change*, *10*(12), 1143–1148.

Nowinski, N. S., Taneva, L., Trumbore, S. E., & Welker, J. M. (2010). Decomposition of old organic matter as a result of deeper active layers in a snow depth manipulation experiment. *Oecologia*, *163*(3), 785–792.

Obu, J., Lantuit, H., Myers-Smith, I., Heim, B., Wolter, J., & Fritz, M. (2017). Effect of terrain characteristics on soil organic carbon and total nitrogen stocks in soils of Herschel Island, Western Canadian Arctic. *Permafrost and Periglacial Processes*, *28*(1), 92–107.

Pearson, R. G., Phillips, S. J., Loranty, M. M., Beck, P. S., Damoulas, T., Knight, S. J., & Goetz, S. J. (2013). Shifts in Arctic vegetation and associated feedbacks under climate change. *Nature Climate Change*, *3*(7), 673–677.

Pebesma, E. J. (2006). The gstat package. *Á Bwww. Gstat. Org*.

Rinnan, R., Michelsen, A., & Jonasson, S. (2008). Effects of litter addition and warming on soil carbon, nutrient pools and microbial communities in a subarctic heath ecosystem. *Applied Soil Ecology*, *39*(3), 271–281.

Rixen, C., Høye, T. T., Macek, P., Aerts, R., Alatalo, J., Andeson, J., Arnold, P., Barrio, I. C., Bjerke, J., Björkman, M. P., Blok, D., Blume-Werry, G., Boike, J., Bokhorst, S., Carbognani, M., Christiansen, C., Convey, P., Cooper, E. J., Cornelissen, J. H. C., … Zong, S. (2022). Winters are changing: Snow effects on Arctic and alpine tundra ecosystems. *Arctic Science*. https://doi.org/10.1139/AS-2020-0058

Sarneel, J. M., Sundqvist, M. K., Molau, U., Björkman, M. P., & Alatalo, J. M. (2020). Decomposition rate and stabilization across six tundra vegetation types exposed to >20 years of warming. *Science of The Total Environment*, *724*, 138304. https://doi.org/10.1016/j.scitotenv.2020.138304

Scharn, R., Little, C. J., Bacon, C. D., Alatalo, J. M., Antonelli, A., Björkman, M. P., Molau, U., Nilsson, R. H., & Björk, R. G. (2021). Decreased soil moisture due to warming drives phylogenetic diversity and community transitions in the tundra. *Environmental Research Letters*, *16*(6), 064031. https://doi.org/10.1088/1748-9326/abfe8a

945 Schuur, E. A., Vogel, J. G., Crummer, K. G., Lee, H., Sickman, J. O., & Osterkamp, T. E. (2009). The
946 effect of permafrost thaw on old carbon release and net carbon exchange from tundra. *Nature*,
947 *459*(7246), 556–559.
948 Shaver, G. R., Giblin, A. E., Nadelhoffer, K. J., Thieler, K. K., Downs, M. R., Laundre, J. A., &
949 Rastetter, E. B. (2006). Carbon turnover in Alaskan tundra soils: Effects of organic matter
950 quality, temperature, moisture and fertilizer. *Journal of Ecology*, *94*(4), 740–753.
951 Sierra, C. A., Trumbore, S. E., Davidson, E. A., Vicca, S., & Janssens, I. (2015). Sensitivity of
952 decomposition rates of soil organic matter with respect to simultaneous changes in
953 temperature and moisture. *Journal of Advances in Modeling Earth Systems*, *7*(1), 335–356.
954 Siewert, M. B., & Olofsson, J. (2020). Scale-dependency of Arctic ecosystem properties revealed by
955 UAV. *Environmental Research Letters*, *15*(9), 094030.
956 Speed, J. D. M., Martinsen, V., Hester, A. J., Holand, Ø., Mulder, J., Mysterud, A., & Austrheim, G.
957 (2015). Continuous and discontinuous variation in ecosystem carbon stocks with elevation
958 across a treeline ecotone. *Biogeosciences*, *12*(5), 1615–1627.
959 Sturm, M., Schimel, J., Michaelson, G., Welker, J. M., Oberbauer, S. F., Liston, G. E., Fahnestock, J.,
960 & Romanovsky, V. E. (2005). Winter biological processes could help convert arctic tundra to
961 shrubland. *Bioscience*, *55*(1), 17–26.
962 Sundqvist, M. K., Giesler, R., & Wardle, D. A. (2011). Within-and across-species responses of plant
963 traits and litter decomposition to elevation across contrasting vegetation types in subarctic
964 tundra. *PloS One*, *6*(10), e27056.
965 Suseela, V., Tharayil, N., Xing, B., & Dukes, J. S. (2013). Labile compounds in plant litter reduce the
966 sensitivity of decomposition to warming and altered precipitation. *New Phytologist*, *200*(1),
967 122–133.
968 Sveinbjörnsson, B., Davis, J., Abadie, W., & Butler, A. (1995). Soil carbon and nitrogen
969 mineralization at different elevations in the Chugach Mountains of south-central Alaska,
970 USA. *Arctic and Alpine Research*, *27*(1), 29–37.
971 Swift, M. J., Heal, O. W., Anderson, J. M., & Anderson, J. M. (1979). *Decomposition in terrestrial*
972 *ecosystems*.
973 Tape, K. E. N., Sturm, M., & Racine, C. (2006). The evidence for shrub expansion in Northern Alaska
974 and the Pan-Arctic. *Global Change Biology*, *12*(4), 686–702.
975 Team, R. C. (2013). *R: A language and environment for statistical computing*.
976 Thakur, M. P., Reich, P. B., Hobbie, S. E., Stefanski, A., Rich, R., Rice, K. E., Eddy, W. C., &
977 Eisenhauer, N. (2018). Reduced feeding activity of soil detritivores under warmer and drier
978 conditions. *Nature Climate Change*, *8*(1), 75–78.
979 Van Gestel, N., Shi, Z., Van Groenigen, K. J., Osenberg, C. W., Andresen, L. C., Dukes, J. S.,
980 Hovenden, M. J., Luo, Y., Michelsen, A., & Pendall, E. (2018). Predicting soil carbon loss
981 with warming. *Nature*, *554*(7693), E4–E5.
982 Wall, D. H., Bradford, M. A., ST. JOHN, M. G., Trofymow, J. A., Behan-Pelletier, V., Bignell, D. E.,
983 Dangerfield, J. M., Parton, W. J., Rusek, J., & Voigt, W. (2008). Global decomposition
984 experiment shows soil animal impacts on decomposition are climate-dependent. *Global*
985 *Change Biology*, *14*(11), 2661–2677.
986 Waring, R. H., & Schlesinger, W. H. (1985). Forest ecosystems. *Analysis at Multiples Scales*, 55.
987 Xue, K., Yuan, M. M., Shi, Z. J., Qin, Y., Deng, Y., Cheng, L., Wu, L., He, Z., Van Nostrand, J. D.,
988 & Bracho, R. (2016). Tundra soil carbon is vulnerable to rapid microbial decomposition
989 under climate warming. *Nature Climate Change*, *6*(6), 595–600.
990 Yi, Y., Kimball, J. S., Chen, R. H., Moghaddam, M., Reichle, R. H., Mishra, U., Zona, D., & Oechel,
991 W. C. (2018). Characterizing permafrost active layer dynamics and sensitivity to landscape
992 spatial heterogeneity in Alaska. *The Cryosphere*, *12*(1), 145–161. https://doi.org/10.5194/tc-
993 12-145-2018
994 Zona, D., Lipson, D. A., Zulueta, R. C., Oberbauer, S. F., & Oechel, W. C. (2011). Microtopographic
995 controls on ecosystem functioning in the Arctic Coastal Plain. *Journal of Geophysical*
996 *Research: Biogeosciences*, *116*(G4). https://doi.org/10.1029/2009JG001241

SUPPLEMENTARY MATERIALS:

Supplementary List 1: List of analyses by research question

1) How do microclimate, microtopography and soil conditions vary spatially across a tundra landscape?

- Bayesian model for each decomposition metric: *decomposition_metric_scaled ~ elevation_scaled, slope_scaled, aspect_class + (1|Plot)*
- Bayesian model without Plot random effect for each decomposition metric: *decomposition_metric_scaled ~ elevation_scaled, slope_scaled, aspect_class*
- Semi-variograms or each decomposition metric, thermal sum, active layer thickness and soil moisture

(2) How does microtopography, microclimate, soil moisture and active layer thickness influence litter decomposition?

- PCA using decomposition metrics, thermal sum, active layer thickness, soil moisture, elevation, slope and aspect as classification variables. 'Plot' was used as a clustering variable.

(3) Do surface microclimate and below-ground microenvironment drivers influence litter decomposition?

- Soil moisture Bayesian model for each decomposition metric: *decomposition_metric_scaled ~ soilmoisture_scaled + thermalsum_scaled + (1|Plot)*
- Active layer Bayesian model for each decomposition metric: *decomposition_metric_scaled ~ activelayer_scaled + thermalsum_scaled + (1|Plot)*
- Bayesian model without Plot random effect for each decomposition metric: *decomposition_metric_scaled ~ activelayer_scaled OR soilmoisture_scaled + thermalsum_scaled*

Supplementary Table 1: Semivariogram Output - dimensions of variogram analysis in *gstat*

Semivariogram ID:	Variogram type	Nugget	Sill	Range
Thermal Sum °C	Exp (Values have been log-transformed)	0.44	7.54	10.50
Active Layer Thickness (mm)	Sph	56.28	114.87	28.51
Soil Moisture %	Mat	69.75	131.55	34.79
Green Tea Mass Loss %	Sph	20.78	39.37	0.00
Rooibos Tea Mass Loss %	Exp	0	8.20	10.43

Supplementary Table 2: Full Model Output (no interactions)

Model Name	Term	Estimate	Std. error	Lower 95% CI	Upper 95% CI
Soil moisture and thermal sum vs Green Tea Mass Loss	bIntercept	0.771	0.37	-0.1	1.417
	bSoilmoistscaled	0.138	0.028	0.083	0.192
	bthermscaled	0.092	0.371	-0.557	0.963
	sdPlotIntercept	0.029	0.021	0.001	0.081
	sigma	0.117	0.007	0.104	0.133
	rPlot[CHHE,Intercept]	0.002	0.028	-0.051	0.069
	rPlot[CHKO,Intercept]	0.009	0.026	-0.038	0.072
	rPlot[DG,Intercept]	-0.02	0.03	-0.094	0.023
	rPlot[ECN,Intercept]	-0.001	0.021	-0.044	0.043
	rPlot[ECS,Intercept]	0.018	0.024	-0.019	0.074
	rPlot[ECW,Intercept]	-0.021	0.026	-0.082	0.018
	rPlot[FO,Intercept]	0.015	0.024	-0.025	0.071
	rPlot[FP,Intercept]	-0.002	0.023	-0.054	0.044
Soil moisture and thermal sum vs Rooibos Tea Mass Loss	bIntercept	0.495	0.602	-0.775	1.667
	bSoilmoistscaled	0.096	0.05	-0.005	0.193
	bthermscaled	0.386	0.605	-0.776	1.679
	sdPlotIntercept	0.067	0.04	0.007	0.163
	sigma	0.165	0.011	0.146	0.188
	rPlot[CHHE,Intercept]	-0.031	0.054	-0.146	0.072
	rPlot[CHKO,Intercept]	0.021	0.049	-0.07	0.131
	rPlot[DG,Intercept]	-0.044	0.054	-0.17	0.042
	rPlot[ECN,Intercept]	0.045	0.043	-0.028	0.14
	rPlot[ECS,Intercept]	-0.003	0.04	-0.088	0.078

	rPlot[ECW,Intercept]	0.014	0.042	-0.068	0.104
	rPlot[FO,Intercept]	0.055	0.051	-0.027	0.167
	rPlot[FP,Intercept]	-0.058	0.052	-0.175	0.021
Soil moisture and thermal sum vs Decomposition Rate	bIntercept	0.783	1.017	-1.102	3.011
	bSoilmoistscaled	-0.001	0.087	-0.175	0.165
	bthermscaled	0.162	1.015	-2.03	2.063
	sdPlotIntercept	0.096	0.067	0.006	0.256
	sigma	0.308	0.02	0.273	0.35
	rPlot[CHHE,Intercept]	-0.026	0.087	-0.225	0.137
	rPlot[CHKO,Intercept]	-0.017	0.077	-0.193	0.131
	rPlot[DG,Intercept]	-0.023	0.079	-0.196	0.132
	rPlot[ECN,Intercept]	0.071	0.074	-0.042	0.241
	rPlot[ECS,Intercept]	-0.041	0.071	-0.201	0.086
	rPlot[ECW,Intercept]	0.075	0.079	-0.041	0.257
	rPlot[FO,Intercept]	0.029	0.075	-0.101	0.204
	rPlot[FP,Intercept]	-0.067	0.08	-0.256	0.058
Soil moisture and thermal sum vs Stabilisation Factor	bIntercept	1.161	0.287	0.67	1.849
	bSoilmoistscaled	-0.108	0.022	-0.152	-0.063
	bthermscaled	-0.071	0.287	-0.75	0.419
	sdPlotIntercept	0.023	0.017	0.001	0.067
	sigma	0.092	0.006	0.081	0.104
	rPlot[CHHE,Intercept]	-0.001	0.022	-0.054	0.039
	rPlot[CHKO,Intercept]	-0.007	0.02	-0.056	0.028
	rPlot[DG,Intercept]	0.016	0.023	-0.017	0.074
	rPlot[ECN,Intercept]	0.001	0.016	-0.033	0.036
	rPlot[ECS,Intercept]	-0.015	0.019	-0.06	0.014
	rPlot[ECW,Intercept]	0.016	0.02	-0.014	0.064
	rPlot[FO,Intercept]	-0.012	0.019	-0.057	0.019

	rPlot[FP,Intercept]	0.002	0.018	-0.034	0.043
Active Layer and thermal sum vs Green Tea Mass Loss	bIntercept	0.904	0.521	-0.275	1.79
	bALTscaled	0.078	0.036	0.008	0.148
	bthermscaled	0.011	0.53	-0.898	1.207
	sdPlotIntercept	0.052	0.03	0.008	0.129
	sigma	0.123	0.008	0.109	0.139
	rPlot[CHHE,Intercept]	0.001	0.043	-0.077	0.102
	rPlot[CHKO,Intercept]	0.02	0.039	-0.048	0.111
	rPlot[DG,Intercept]	-0.056	0.046	-0.164	0.012
	rPlot[ECN,Intercept]	0.028	0.033	-0.03	0.099
	rPlot[ECS,Intercept]	0.01	0.031	-0.051	0.077
	rPlot[ECW,Intercept]	-0.009	0.033	-0.083	0.052
	rPlot[FO,Intercept]	0.041	0.037	-0.024	0.118
	rPlot[FP,Intercept]	-0.037	0.038	-0.123	0.024
Active Layer and thermal sum vs Rooibos Tea Mass Loss	bIntercept	0.597	0.771	-0.988	2.09
	bALTscaled	0.023	0.05	-0.077	0.122
	bthermscaled	0.35	0.782	-1.158	1.969
	sdPlotIntercept	0.103	0.042	0.045	0.21
	sigma	0.165	0.01	0.146	0.187
	rPlot[CHHE,Intercept]	-0.046	0.072	-0.192	0.101
	rPlot[CHKO,Intercept]	0.032	0.064	-0.089	0.166
	rPlot[DG,Intercept]	-0.075	0.066	-0.214	0.047
	rPlot[ECN,Intercept]	0.075	0.052	-0.026	0.184
	rPlot[ECS,Intercept]	-0.019	0.052	-0.124	0.081
	rPlot[ECW,Intercept]	0.033	0.054	-0.072	0.143
	rPlot[FO,Intercept]	0.096	0.059	-0.013	0.22
	rPlot[FP,Intercept]	-0.099	0.059	-0.226	0.008

Active Layer and thermal sum vs Decomposition Rate	bIntercept	0.533	1.006	-1.335	2.667
	bALTscaled	-0.084	0.088	-0.257	0.089
	bthermscaled	0.492	1.033	-1.68	2.425
	sdPlotIntercept	0.088	0.058	0.007	0.228
	sigma	0.308	0.02	0.273	0.349
	rPlot[CHHE,Intercept]	-0.023	0.08	-0.203	0.125
	rPlot[CHKO,Intercept]	-0.012	0.072	-0.172	0.128
	rPlot[DG,Intercept]	-0.021	0.073	-0.176	0.124
	rPlot[ECN,Intercept]	0.056	0.068	-0.055	0.214
	rPlot[ECS,Intercept]	-0.04	0.065	-0.187	0.073
	rPlot[ECW,Intercept]	0.064	0.072	-0.048	0.228
	rPlot[FO,Intercept]	0.039	0.073	-0.086	0.204
	rPlot[FP,Intercept]	-0.059	0.073	-0.225	0.059
Active Layer and thermal sum vs Stabilisation Factor	bIntercept	1.113	0.513	0.378	2.356
	bALTscaled	-0.06	0.029	-0.115	-0.004
	bthermscaled	-0.066	0.524	-1.322	0.692
	sdPlotIntercept	0.043	0.026	0.008	0.113
	sigma	0.096	0.006	0.086	0.109
	rPlot[CHHE,Intercept]	-0.004	0.04	-0.115	0.06
	rPlot[CHKO,Intercept]	-0.018	0.034	-0.109	0.036
	rPlot[DG,Intercept]	0.047	0.04	-0.009	0.156
	rPlot[ECN,Intercept]	-0.022	0.026	-0.077	0.026
	rPlot[ECS,Intercept]	-0.008	0.024	-0.056	0.04
	rPlot[ECW,Intercept]	0.01	0.028	-0.04	0.078
	rPlot[FO,Intercept]	-0.032	0.028	-0.091	0.019
	rPlot[FP,Intercept]	0.032	0.031	-0.017	0.106

Topography vs Green Tea Mass Loss	bIntercept	1.007	0.051	0.905	1.104
	belevationscaled	-0.003	0.036	-0.079	0.062
	bslopescaled	-0.018	0.025	-0.066	0.03
	baspectclassNorth	0.121	0.052	0.021	0.224
	baspectclassSouth	-0.022	0.036	-0.091	0.053
	baspectclassWest	-0.004	0.038	-0.075	0.073
	sdPlotIntercept	0.033	0.025	0.002	0.096
	sigma	0.122	0.008	0.109	0.138
	rPlot[CHHE,Intercept]	-0.009	0.03	-0.074	0.051
	rPlot[CHKO,Intercept]	0.009	0.03	-0.046	0.077
	rPlot[DG,Intercept]	-0.029	0.037	-0.121	0.019
	rPlot[ECN,Intercept]	0.014	0.025	-0.029	0.071
	rPlot[ECS,Intercept]	0.003	0.028	-0.052	0.067
	rPlot[ECW,Intercept]	0.004	0.025	-0.049	0.058
	rPlot[FO,Intercept]	0.015	0.035	-0.044	0.095
	rPlot[FP,Intercept]	-0.007	0.026	-0.067	0.043
Topography vs Rooibos Tea Mass Loss	bIntercept	1.074	0.11	0.85	1.291
	belevationscaled	-0.083	0.093	-0.283	0.094
	bslopescaled	-0.017	0.046	-0.104	0.076
	baspectclassNorth	-0.028	0.08	-0.184	0.132
	baspectclassSouth	-0.035	0.064	-0.16	0.093
	baspectclassWest	-0.007	0.065	-0.136	0.121
	sdPlotIntercept	0.12	0.06	0.046	0.28
	sigma	0.183	0.012	0.162	0.208
	rPlot[CHHE,Intercept]	-0.028	0.091	-0.2	0.16
	rPlot[CHKO,Intercept]	0.045	0.086	-0.11	0.231

	rPlot[DG,Intercept]	-0.113	0.092	-0.313	0.045
	rPlot[ECN,Intercept]	0.081	0.065	-0.038	0.216
	rPlot[ECS,Intercept]	-0.026	0.075	-0.176	0.125
	rPlot[ECW,Intercept]	0.034	0.067	-0.104	0.163
	rPlot[FO,Intercept]	0.089	0.095	-0.095	0.29
	rPlot[FP,Intercept]	-0.079	0.071	-0.233	0.046
Topography vs Decomposition Rate	bIntercept	1.018	0.148	0.722	1.307
	belevationscaled	-0.036	0.107	-0.24	0.185
	bslopescaled	0.018	0.069	-0.116	0.161
	baspectclassNorth	-0.135	0.133	-0.4	0.124
	baspectclassSouth	-0.047	0.1	-0.247	0.145
	baspectclassWest	-0.091	0.104	-0.302	0.11
	sdPlotIntercept	0.125	0.072	0.021	0.305
	sigma	0.307	0.02	0.271	0.348
	rPlot[CHHE,Intercept]	-0.016	0.1	-0.224	0.19
	rPlot[CHKO,Intercept]	0.013	0.097	-0.179	0.217
	rPlot[DG,Intercept]	-0.024	0.1	-0.23	0.189
	rPlot[ECN,Intercept]	0.097	0.084	-0.042	0.28
	rPlot[ECS,Intercept]	-0.084	0.102	-0.316	0.086
	rPlot[ECW,Intercept]	0.068	0.084	-0.088	0.249
	rPlot[FO,Intercept]	0.033	0.111	-0.184	0.273
	rPlot[FP,Intercept]	-0.094	0.092	-0.297	0.064
Topography vs Stabilisation Factor	bIntercept	0.975	0.038	0.9	1.052
	belevationscaled	0.005	0.03	-0.045	0.084
	bslopescaled	0.014	0.019	-0.024	0.052
	baspectclassNorth	-0.095	0.041	-0.174	-0.013

	baspectclassSouth	0.017	0.029	-0.042	0.072
	baspectclassWest	0.003	0.03	-0.058	0.06
	sdPlotIntercept	0.028	0.022	0.001	0.085
	sigma	0.096	0.006	0.085	0.108
	rPlot[CHHE,Intercept]	0.005	0.027	-0.058	0.06
	rPlot[CHKO,Intercept]	-0.009	0.027	-0.074	0.037
	rPlot[DG,Intercept]	0.025	0.03	-0.014	0.1
	rPlot[ECN,Intercept]	-0.013	0.022	-0.062	0.023
	rPlot[ECS,Intercept]	-0.004	0.025	-0.067	0.042
	rPlot[ECW,Intercept]	-0.003	0.02	-0.045	0.039
	rPlot[FO,Intercept]	-0.011	0.026	-0.07	0.036
	rPlot[FP,Intercept]	0.005	0.021	-0.035	0.056

Supplementary Table 3: Model Output (no random effect, no interactions)

Model name	Term	Estimate	Std. error	Lower 95% CI	Upper 95% CI
Soil moisture & surface temperature vs Green Tea Mass Loss	b_Intercept	0.858	0.224	0.415	1.295
	b_Soilmoist_scaled	0.141	0.025	0.091	0.191
	b_therm_scaled	0.001	0.225	-0.439	0.438
	sigma	0.118	0.007	0.105	0.133
Soil moisture & surface temperature vs Rooibos Tea Mass Loss	b_Intercept	0.364	0.36	-0.345	1.077
	b_Soilmoist_scaled	0.181	0.041	0.1	0.26
	b_therm_scaled	0.447	0.36	-0.263	1.154
	sigma	0.189	0.011	0.168	0.213
Soil moisture & surface temperature vs Decomposition Rate	b_Intercept	0.503	0.598	-0.67	1.685
	b_Soilmoist_scaled	0.063	0.069	-0.072	0.2
	b_therm_scaled	0.389	0.599	-0.787	1.564
	sigma	0.312	0.019	0.277	0.352
Soil moisture & surface temperature vs Stabilisation Factor	b_Intercept	1.092	0.176	0.753	1.443
	b_Soilmoist_scaled	-0.111	0.02	-0.15	-0.072
	b_therm_scaled	0.001	0.176	-0.35	0.344
	sigma	0.093	0.006	0.083	0.104
Active Layer & surface temperature vs Green Tea Mass Loss	b_Intercept	1.212	0.266	0.691	1.729
	b_ALT_scaled	0.087	0.033	0.022	0.153
	b_therm_scaled	-0.306	0.279	-0.845	0.246
	sigma	0.127	0.008	0.113	0.143
Active Layer & surface temperature vs Rooibos Tea Mass Loss	b_Intercept	0.673	0.382	-0.082	1.417
	b_ALT_scaled	0.032	0.047	-0.06	0.123
	b_therm_scaled	0.27	0.399	-0.513	1.055
	sigma	0.18	0.011	0.159	0.203
Active Layer & surface temperature vs Decomposition Rate	b_Intercept	0.291	0.661	-1.008	1.593
	b_ALT_scaled	-0.099	0.082	-0.258	0.062
	b_therm_scaled	0.752	0.694	-0.609	2.118
	sigma	0.313	0.02	0.278	0.355
Active Layer & surface temperature vs Stabilisation Factor	b_Intercept	0.814	0.208	0.408	1.224
	b_ALT_scaled	-0.068	0.026	-0.12	-0.018
	b_therm_scaled	0.241	0.219	-0.191	0.672

	sigma	0.1	0.006	0.088	0.112
Topography vs Green Tea Mass Loss	b_Intercept	1.024	0.037	0.951	1.097
	b_elevation_scaled	-0.006	0.021	-0.047	0.035
	b_slope_scaled	-0.026	0.019	-0.064	0.012
	b_aspect_classNorth	0.106	0.044	0.021	0.191
	b_aspect_classSouth	-0.032	0.027	-0.085	0.021
	b_aspect_classWest	-0.023	0.03	-0.082	0.035
	sigma	0.124	0.008	0.111	0.14
Topography vs Rooibos Tea Mass Loss	b_Intercept	1.097	0.061	0.976	1.218
	b_elevation_scaled	-0.076	0.034	-0.143	-0.009
	b_slope_scaled	-0.024	0.031	-0.086	0.038
	b_aspect_classNorth	0.046	0.073	-0.097	0.19
	b_aspect_classSouth	-0.07	0.043	-0.154	0.016
	b_aspect_classWest	-0.043	0.048	-0.137	0.051
	sigma	0.196	0.012	0.174	0.221
Topography vs Decomposition Rate	b_Intercept	0.972	0.102	0.773	1.175
	b_elevation_scaled	-0.053	0.057	-0.167	0.058
	b_slope_scaled	0.014	0.051	-0.087	0.114
	b_aspect_classNorth	-0.017	0.119	-0.248	0.214
	b_aspect_classSouth	0.018	0.07	-0.121	0.155
	b_aspect_classWest	0.011	0.079	-0.145	0.165
	sigma	0.316	0.02	0.28	0.357
Topography vs Stabilisation Factor	b_Intercept	0.964	0.03	0.905	1.022
	b_elevation_scaled	0.005	0.016	-0.027	0.037
	b_slope_scaled	0.02	0.015	-0.009	0.049
	b_aspect_classNorth	-0.083	0.035	-0.151	-0.016
	b_aspect_classSouth	0.025	0.021	-0.017	0.067
	b_aspect_classWest	0.017	0.024	-0.029	0.064
	sigma	0.097	0.006	0.086	0.11

Supplementary Table 4: Full Model Output (with interactions)

Model name	Term	Estimate	Std. error	Lower 95% CI	Upper 95% CI
Soil moisture and thermal sum vs Green Tea Mass Loss	bIntercept	1.197	0.666	-0.197	2.464
	bSoilmoistscaled	-0.363	0.656	-1.655	0.925
	bthermscaled	-0.334	0.666	-1.603	1.056
	bSoilmoistscaled:thermscaled	0.501	0.656	-0.786	1.795
	sdPlotIntercept	0.029	0.022	0.002	0.082
	sigma	0.117	0.007	0.104	0.132
	rPlot[CHHE,Intercept]	0	0.028	-0.05	0.066
	rPlot[CHKO,Intercept]	0.01	0.026	-0.035	0.074
	rPlot[DG,Intercept]	-0.018	0.029	-0.089	0.024
	rPlot[ECN,Intercept]	-0.001	0.021	-0.046	0.042
	rPlot[ECS,Intercept]	0.018	0.024	-0.019	0.076
	rPlot[ECW,Intercept]	-0.021	0.026	-0.084	0.016
	rPlot[FO,Intercept]	0.012	0.024	-0.03	0.069
	rPlot[FP,Intercept]	-0.001	0.023	-0.053	0.047
Soil moisture and thermal sum vs Rooibos Tea Mass Loss	bIntercept	0.576	1.04	-1.535	2.556
	bSoilmoistscaled	0.035	0.992	-1.854	2
	bthermscaled	0.304	1.046	-1.668	2.442
	bSoilmoistscaled:thermscaled	0.061	0.998	-1.916	1.967
	sdPlotIntercept	0.066	0.041	0.007	0.167
	sigma	0.166	0.011	0.146	0.189
	rPlot[CHHE,Intercept]	-0.032	0.055	-0.152	0.072
	rPlot[CHKO,Intercept]	0.019	0.049	-0.074	0.127

	rPlot[DG,Intercept]	-0.042	0.054	-0.165	0.047
	rPlot[ECN,Intercept]	0.045	0.044	-0.026	0.144
	rPlot[ECS,Intercept]	-0.002	0.042	-0.089	0.083
	rPlot[ECW,Intercept]	0.016	0.043	-0.065	0.109
	rPlot[FO,Intercept]	0.056	0.053	-0.026	0.176
	rPlot[FP,Intercept]	-0.056	0.052	-0.174	0.025
Soil moisture and thermal sum vs Decomposition Rate	bIntercept	0.497	1.833	-3.102	4.07
	bSoilmoistscaled	0.339	1.856	-3.414	4.024
	bthermscaled	0.453	1.839	-3.124	4.085
	bSoilmoistscaled:thermscaled	-0.342	1.865	-4.036	3.414
	sdPlotIntercept	0.099	0.069	0.007	0.265
	sigma	0.31	0.02	0.274	0.352
	rPlot[CHHE,Intercept]	-0.027	0.09	-0.238	0.131
	rPlot[CHKO,Intercept]	-0.02	0.079	-0.2	0.128
	rPlot[DG,Intercept]	-0.028	0.081	-0.212	0.128
	rPlot[ECN,Intercept]	0.07	0.075	-0.045	0.244
	rPlot[ECS,Intercept]	-0.042	0.073	-0.206	0.08
	rPlot[ECW,Intercept]	0.076	0.081	-0.045	0.263
	rPlot[FO,Intercept]	0.033	0.078	-0.1	0.215
	rPlot[FP,Intercept]	-0.073	0.086	-0.27	0.058
Soil moisture and thermal sum vs Stabilisation Factor	bIntercept	0.83	0.528	-0.167	1.878
	bSoilmoistscaled	0.285	0.526	-0.739	1.31
	bthermscaled	0.261	0.528	-0.795	1.259
	bSoilmoistscaled:thermscaled	-0.394	0.526	-1.42	0.626
	sdPlotIntercept	0.023	0.018	0.001	0.065
	sigma	0.092	0.006	0.082	0.104

	rPlot[CHHE,Intercept]	0	0.022	-0.05	0.041
	rPlot[CHKO,Intercept]	-0.007	0.021	-0.057	0.027
	rPlot[DG,Intercept]	0.014	0.023	-0.019	0.074
	rPlot[ECN,Intercept]	0.001	0.017	-0.033	0.036
	rPlot[ECS,Intercept]	-0.014	0.019	-0.059	0.016
	rPlot[ECW,Intercept]	0.017	0.021	-0.013	0.069
	rPlot[FO,Intercept]	-0.01	0.019	-0.054	0.025
	rPlot[FP,Intercept]	0.001	0.019	-0.036	0.043
Active Layer and thermal sum vs Green Tea Mass Loss	bIntercept	1.45	0.908	-0.389	3.209
	bALTscaled	-0.618	0.871	-2.33	1.075
	bthermscaled	-0.536	0.915	-2.303	1.325
	bALTscaled:thermscaled	0.691	0.865	-0.99	2.39
	sdPlotIntercept	0.058	0.032	0.012	0.135
	sigma	0.122	0.008	0.108	0.139
	rPlot[CHHE,Intercept]	-0.003	0.046	-0.088	0.103
	rPlot[CHKO,Intercept]	0.025	0.042	-0.047	0.117
	rPlot[DG,Intercept]	-0.065	0.048	-0.172	0.008
	rPlot[ECN,Intercept]	0.032	0.035	-0.03	0.105
	rPlot[ECS,Intercept]	0.013	0.033	-0.049	0.081
	rPlot[ECW,Intercept]	-0.008	0.036	-0.085	0.056
	rPlot[FO,Intercept]	0.042	0.038	-0.024	0.121
	rPlot[FP,Intercept]	-0.04	0.04	-0.128	0.025
Active Layer and thermal sum vs Rooibos Tea Mass Loss	bIntercept	-0.665	1.274	-3.181	1.839
	bALTscaled	1.486	1.186	-0.841	3.792
	bthermscaled	1.616	1.283	-0.902	4.154
	bALTscaled:thermscaled	-1.456	1.18	-3.756	0.85
	sdPlotIntercept	0.099	0.045	0.041	0.213
	sigma	0.165	0.011	0.146	0.187

	rPlot[CHHE,Intercept]	-0.032	0.071	-0.176	0.114
	rPlot[CHKO,Intercept]	0.028	0.062	-0.094	0.158
	rPlot[DG,Intercept]	-0.067	0.064	-0.204	0.05
	rPlot[ECN,Intercept]	0.069	0.052	-0.029	0.176
	rPlot[ECS,Intercept]	-0.024	0.051	-0.126	0.076
	rPlot[ECW,Intercept]	0.027	0.053	-0.08	0.134
	rPlot[FO,Intercept]	0.098	0.058	-0.01	0.219
	rPlot[FP,Intercept]	-0.099	0.058	-0.221	0.005
Active Layer and thermal sum vs Decomposition Rate	bIntercept	-3.016	2.015	-6.896	0.975
	bALTscaled	4.112	2.124	-0.028	8.21
	bthermscaled	4.046	2.03	0.037	7.953
	bALTscaled:thermscaled	-4.171	2.11	-8.247	-0.049
	sdPlotIntercept	0.082	0.056	0.005	0.218
	sigma	0.305	0.019	0.269	0.346
	rPlot[CHHE,Intercept]	0.001	0.075	-0.161	0.158
	rPlot[CHKO,Intercept]	-0.018	0.068	-0.174	0.113
	rPlot[DG,Intercept]	-0.009	0.069	-0.158	0.133
	rPlot[ECN,Intercept]	0.045	0.064	-0.062	0.193
	rPlot[ECS,Intercept]	-0.049	0.065	-0.2	0.056
	rPlot[ECW,Intercept]	0.049	0.067	-0.059	0.202
	rPlot[FO,Intercept]	0.041	0.069	-0.074	0.201
	rPlot[FP,Intercept]	-0.058	0.071	-0.224	0.053
Active Layer and thermal sum vs Stabilisation Factor	bIntercept	0.638	0.704	-0.701	2.055
	bALTscaled	0.462	0.682	-0.882	1.805
	bthermscaled	0.412	0.709	-1.02	1.768
	bALTscaled:thermscaled	-0.52	0.678	-1.86	0.811
	sdPlotIntercept	0.044	0.026	0.008	0.107
	sigma	0.096	0.006	0.085	0.109

	rPlot[CHHE,Intercept]	0.002	0.035	-0.077	0.066
	rPlot[CHKO,Intercept]	-0.019	0.032	-0.094	0.035
	rPlot[DG,Intercept]	0.049	0.038	-0.009	0.135
	rPlot[ECN,Intercept]	-0.025	0.027	-0.082	0.023
	rPlot[ECS,Intercept]	-0.011	0.026	-0.064	0.039
	rPlot[ECW,Intercept]	0.006	0.027	-0.046	0.063
	rPlot[FO,Intercept]	-0.033	0.029	-0.094	0.018
	rPlot[FP,Intercept]	0.03	0.031	-0.021	0.1

1056

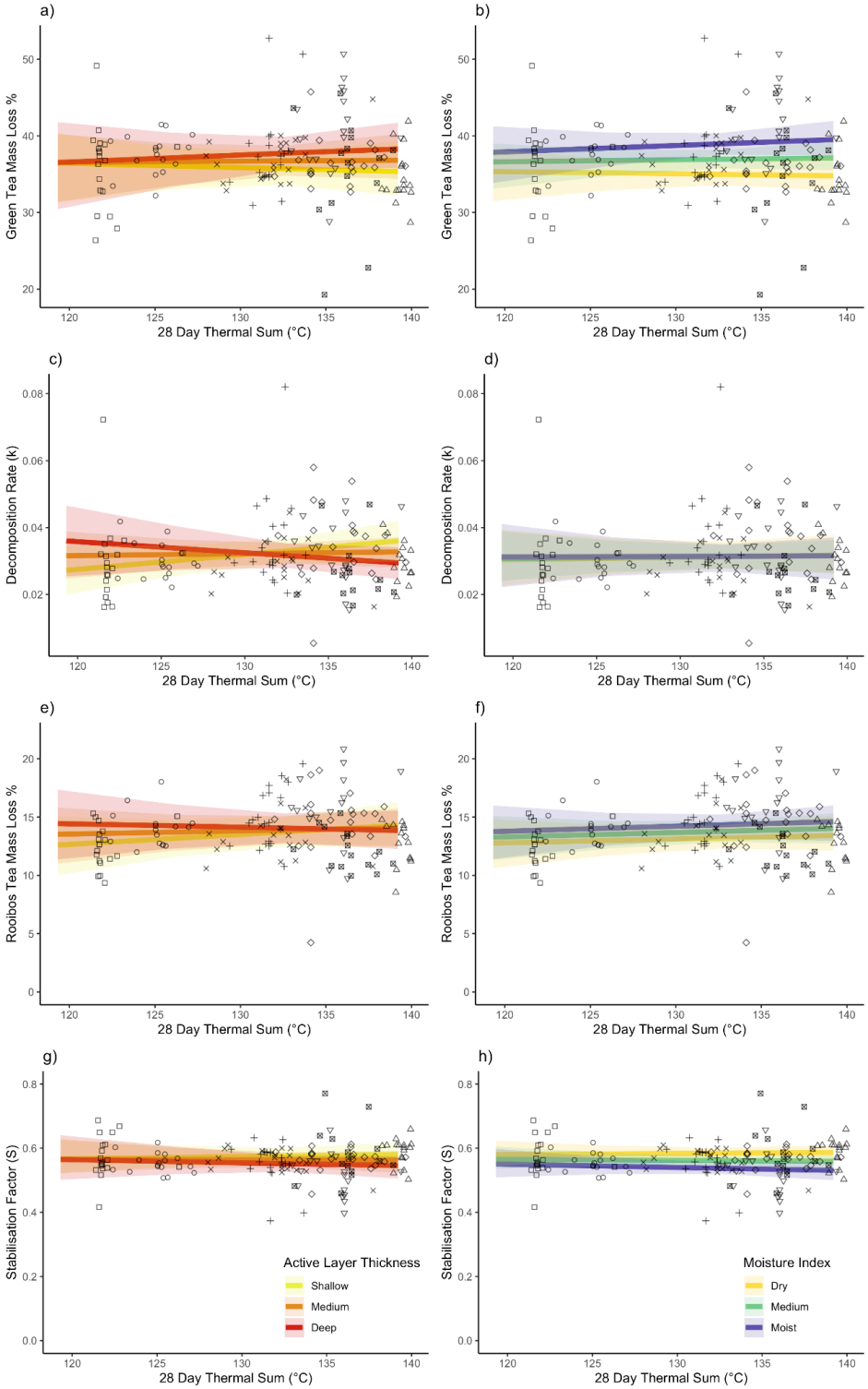

Supplementary Figure 1: *Increased soil moisture corresponded with higher green and rooibos tea mass loss, lower stabilisation rate and did not explain decomposition rate (b,d,f,h). The relationship between decomposition rate and temperature was weakly positive for shallow active layers and weakly negative for deep active layers with decomposition being faster where the active layer was deeper in cooler microclimates, and slower in areas with deeper activer layers but warmer surface temperatures - while no trend is apparent between soil moisture and decomposition rates. The trend lines are Bayesian model fits with ribbons showing 95% credible intervals. Trend lines and ribbon colours represent categories of dry, medium and moist soils (left panel) and shallow, medium and deep active layers (right panel). Full outputs can be found in Table S3.*